Materials Advances

ROYAL SOCIETY OF CHEMISTRY

REVIEW

View Article Online
View Journal | View Issue

Cite this: *Mater. Adv.*, 2024, 5, 4996

Innovative approaches in skin therapy: bionanocomposites for skin tissue repair and regeneration

Ayça Bal-Öztürk,[abc] Emine Alarçin,[d] Gökçen Yaşayan,[e] Meltem Avci-Adali,[f] Arezoo Khosravi,[g] Atefeh Zarepour,[h] Siavash Iravani *[i] and Ali Zarrabi *[jk]

Bionanocomposites (BNCs) have gained significant attention in the field of biomaterials, particularly for their potential applications in skin tissue repair and regeneration. Advantages of these biomaterials in skin care and wound healing/dressings include their ability to provide a suitable environment for tissue regeneration. They can mimic the extracellular matrix, supporting cellular interactions and promoting the formation of new tissue. They can also be engineered to have controlled release properties, allowing for the localized and sustained delivery of bioactive molecules, growth factors, or antimicrobial agents to the wound site. BNCs can be used as scaffolds or matrices for bioprinting, enabling the fabrication of complex structures that closely resemble native tissue. BNC-based films, hydrogels, and dressings can serve as protective barriers, promoting an optimal wound healing environment and preventing infection. These materials can also be incorporated into advanced wound care products, such as smart dressings, which can monitor wound healing progress and provide real-time feedback to healthcare professionals. This review aims to provide a comprehensive overview of the current trends, advantages, challenges, and future directions in this rapidly evolving field. The current trends in the field are deliberated, including the incorporation of natural polymers, such as silk fibroin, hyaluronic acid, collagen, gelatin, chitosan/chitin, alginate, starch, bacterial cellulose, among others. These BNCs offer biocompatibility/biodegradability, enhanced mechanical strength, and the ability to promote cell adhesion and proliferation. However, crucial challenges such as biocompatibility optimization, mechanical property tuning, and regulatory approval need to be addressed. Furthermore, the future directions and emerging research areas are deliberated, including the development of biomimetic BNCs that mimic the native tissue microenvironment in terms of composition, structure, and bioactive cues. Furthermore, the integration of advanced fabrication techniques, such as 3D bioprinting and electrospinning, and the incorporation of nanoparticles and bioactive molecules hold promise for enhancing the therapeutic efficacy of BNCs in skin tissue repair and regeneration.

Received 13th April 2024,
Accepted 30th May 2024

DOI: 10.1039/d4ma00384e

rsc.li/materials-advances

1. Introduction

In recent years, the field of tissue engineering and regenerative medicine has witnessed tremendous advancements, particularly in the area of skin tissue repair and regeneration. In this context, bionanocomposites (BNCs) have shown promising potential in developing wound care and tissue regeneration (Fig. 1).[1] Typically, they are materials composed of a biopolymer matrix and

[a] *Department of Analytical Chemistry, Faculty of Pharmacy, Istinye University, 34010 Istanbul, Türkiye*
[b] *Institute of Health Sciences, Department of Stem Cell and Tissue Engineering, Istinye University, 34010 Istanbul, Türkiye*
[c] *Stem Cell and Tissue Engineering Application and Research Center (ISUKOK), Istinye University, Istanbul, Türkiye*
[d] *Department of Pharmaceutical Technology, Faculty of Pharmacy, Marmara University, 34854 Istanbul, Türkiye*
[e] *Department of Pharmaceutical Technology, Faculty of Pharmacy, Yeditepe University, 34755 Istanbul, Türkiye*
[f] *Department of Thoracic and Cardiovascular Surgery, University Hospital Tübingen, 72076 Tübingen, Germany*
[g] *Department of Genetics and Bioengineering, Faculty of Engineering and Natural Sciences, Istanbul Okan University, Istanbul 34959, Türkiye*
[h] *Department of Research Analytics, Saveetha Dental College and Hospitals, Saveetha Institute of Medical and Technical Sciences, Saveetha University, Chennai 600 077, India*
[i] *Independent Researcher, W Nazar ST, Boostan Ave, Isfahan, Iran. E-mail: siavashira@gmail.com*
[j] *Department of Biomedical Engineering, Faculty of Engineering and Natural Sciences, Istinye University, Sariyer, 34396 Istanbul, Türkiye. E-mail: alizarrabi@gmail.com*
[k] *Graduate School of Biotechnology and Bioengineering, Yuan Ze University, Taoyuan 320315, Taiwan*

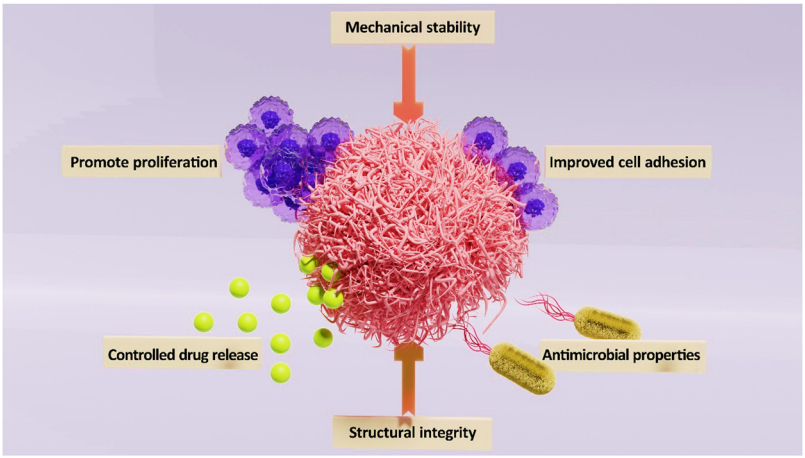

Fig. 1 BNCs for skin tissue repair and regeneration.

nano-sized fillers, such as nanoparticles (NPs) or nanofibers. The biopolymer matrix provides structural integrity and mechanical stability, while the NPs offer enhanced functionalities, such as improved cell adhesion, controlled drug release, and antimicrobial properties. The synergistic combination of these components makes BNCs an ideal choice for skin tissue repair and regeneration.[2,3] One of the key advantages of BNCs is their ability to promote cell adhesion and proliferation. The surface properties of nanomaterials, such as their high surface-to-volume ratio and unique surface chemistry, facilitate cell attachment and spreading. This promotes the formation of new tissue and accelerates the healing process. For instance, soft BNCs composed of polyampholyte and nanosilicate exhibited tunable mechanical, cell adhesion, and degradation properties, serving as suitable scaffolds for tissue engineering.[4] Furthermore, BNCs can be designed to mimic the natural extracellular matrix (ECM), providing a favorable microenvironment for cell growth and differentiation.[5] Another significant benefit of BNCs is their potential for controlled drug delivery.[6,7] By incorporating therapeutic agents or NPs with drug-loading capabilities into the biopolymer matrix, BNCs can release therapeutic agents in a controlled manner. This allows for targeted drug delivery to the site of injury, minimizing side effects and optimizing the healing process;[6,8] the release kinetics can be tailored to match the specific requirements of the wound, ensuring optimal treatment outcomes. Notably, infections are a common complication in skin tissue repair and regeneration. BNCs can address this issue by incorporating antimicrobial agents/NPs, such as silver, TiO_2, or zinc oxide NPs (ZnO), into the biopolymer matrix.[9] These NPs exhibit potent antimicrobial activity, effectively preventing bacterial colonization and promoting wound healing. The use of BNCs with antimicrobial properties can significantly reduce the risk of infection and improve patient outcomes.[9,10]

In the field of skin wound repair and regeneration, various materials and techniques are utilized to enhance the healing process, including traditional approaches such as the use of polymer fibers-based wound dressings containing therapeutic agents or NPs. The challenges such as limited efficacy and potential adverse reactions have led to the exploration of more advanced techniques. One advanced technique is the development of Janus-type biomimetic fabrics with antigravity liquid transport properties.[11] Innovative Janus-type biomimetic fabrics, designed with antigravity unidirectional liquid transport capabilities, play a pivotal role in enhancing wound healing processes. These fabrics facilitate the removal of biofluid from the wound bed while preserving an optimal moisture level. Drawing inspiration from the transpiration mechanism observed in plants, where water is transported from the roots to the leaves and subsequently evaporates, these fabrics mimic nature's efficiency. The distinct feature of asymmetric wettability in Janus fabric, with one side being hydrophilic and the other hydrophobic, generates a compelling force for directing unidirectional liquid transport.[11,12] By harnessing this unique property, researchers aim to create wound dressings that can effectively manage exudate and promote faster healing. The incorporation of such cutting-edge technologies holds great promise for improving outcomes in skin wound repair and regeneration. In one study, a novel biomimetic fabric, drawing inspiration from natural transpiration mechanisms in plants, was unveiled.[13] This fabric ingeniously merged a commercial polyethylene terephthalate fabric with asymmetrical growth of one-dimensional rutile titanium dioxide (TiO_2) micro/nanostructures. It exhibited essential plant characteristics, such as hierarchically porous networks and hydrophilic water conduction channels. This unique structure granted the fabric unparalleled antigravity wicking-evaporation capabilities. The fabric showcased a remarkable 780% one-way transport capacity and a water evaporation rate of 0.75 g h^{-1}, far exceeding that of traditional moisture-wicking textiles. Notably, the integration of one-dimensional rutile TiO_2 micro/nanostructures introduced solar-light triggered antibacterial properties, crucial for dismantling and eliminating wound biofilms. The biomimetic transpiration fabric proved instrumental in draining exudate and eradicating biofilms in *Staphylococcus aureus*-infected wounds. It demonstrated a substantially faster infection eradication potential in comparison to the commonly used ciprofloxacin

irrigation method.[13] These significant findings paved the way for the development of high-performance textile-based wound dressings. These dressings offered efficient clinical solutions to combat biofilms associated with chronic wounds, marking a notable advancement in wound care technology.

When it comes to BNC scaffolds, the design principles revolve around incorporating nanomaterials into biocompatible matrices to enhance the scaffold's mechanical properties, bioactivity, and biodegradability.[6,14,15] By combining nanomaterials such as NPs, nanofibers, or nanotubes with natural or synthetic polymers, researchers aim to create scaffolds that closely mimic the extracellular matrix of tissues. These BNC scaffolds offer a supportive structure for cell attachment, proliferation, and differentiation in tissue engineering applications. The design process typically involves optimizing the composition, morphology, and distribution of nanomaterials within the scaffold to achieve desired mechanical strength, porosity, and bioactive properties. Notably, surface modifications can be implemented to promote cell adhesion and tissue regeneration. By carefully tailoring the nanocomposite scaffold's properties, researchers can create a biomimetic environment that facilitates the regeneration of damaged tissues.[9] BNCs, composed of natural polymers such as silk fibroin, hyaluronic acid, collagen, gelatin, chitosan/chitin, alginate, starch, bacterial cellulose, and more, exhibit a wide range of properties that make them highly suitable for skin tissue repair and regeneration.[16] Their unique characteristics, such as mechanical strength, biodegradability, moisture retention, cellular interactions, antimicrobial properties, gel-forming capabilities, and fibrous structure, contribute to their versatility and potential in the field of tissue engineering and regenerative medicine.[17,18] For instance, silk fibroin is renowned for its remarkable mechanical strength, biocompatibility, and biodegradability.[19] Incorporating silk fibroin into BNCs not only imparts structural integrity and support to the regenerated tissue but also ensures gradual degradation of the BNC scaffold, allowing the regenerated tissue to assume its functionality. Silk fibroin exhibits exceptional absorbent properties, and its versatility enables the formation of diverse materials at different scales, including macro, micro, and nano, such as nanofibers, NPs, hydrogels, and microspheres. The incorporation of inorganic NPs with silk fibroin has gained significant attention, offering enhanced functionalities and value addition. BNCs incorporating silk fibroin have been extensively investigated for tissue replacement applications, such as tendon, corneal stroma, bone, and dermis, owing to their exceptional biocompatibility.[19] In addition, hyaluronic acid, a naturally occurring polysaccharide, is known for its exceptional water-binding capacity and biocompatibility. When integrated into BNCs, hyaluronic acid provides excellent hydration and lubrication properties, making it beneficial for wound healing and tissue regeneration. Its ability to create a favorable microenvironment for cell growth and migration is also advantageous in promoting skin regeneration.[18,20]

Collagen and gelatin, derived from animal sources, are widely recognized for their biocompatibility and bioactivity.[21] These proteins provide a favorable environment for cell adhesion, proliferation, and tissue regeneration. When incorporated into BNCs, collagen and gelatin enhance the biocompatibility of scaffolds, promoting cellular interactions and facilitating the regeneration of skin tissue.[22] Furthermore, chitosan and chitin, derived from crustacean shells, possess antimicrobial properties that can prevent infection during the healing process.[23] They exhibit excellent wound healing properties, promoting cell growth and angiogenesis. When combined with NPs, chitosan/chitin BNCs offer a dual-action approach, protecting against bacterial colonization and accelerating the healing of skin tissue.[23,24] In addition, alginate, starch, and bacterial cellulose are polysaccharides known for their biocompatibility and biodegradability. When utilized in BNCs, they provide structural integrity, promote cell attachment, and regulate the release of bioactive molecules. These properties are essential for skin tissue repair and regeneration, as they assist in wound healing, neovascularization, and extracellular matrix formation.[16,25]

BNCs have shown immense potential in promoting angiogenesis by incorporating NPs that can release growth factors or stimulate the expression of angiogenic proteins. They can create a favorable microenvironment that encourages the growth of new blood vessels, thereby enhancing the supply of oxygen and nutrients to the healing tissue.[16,25] The skin barrier function is essential for protecting the body from external pathogens and maintaining proper hydration.[26] BNCs can play a pivotal role in restoring and improving the skin barrier function through their unique properties. By modulating the composition and structure of the biopolymer matrix, BNCs can mimic the natural skin barrier and regulate transdermal water loss. This helps to prevent excessive moisture loss and maintain optimal hydration levels, facilitating the healing process. For instance, the integration of chitin nanofibrils into poly(lactic acid) (PLA)-based BNCs exhibited significant antimicrobial activity, rendering them suitable for the development of skin-compatible films aimed at wound healing applications.[27] Besides, BNCs offer a platform for enhanced cellular interactions during the repair and regeneration process. The incorporation of NPs with bioactive properties, such as cell adhesion molecules, can facilitate cell attachment and communication. This fosters the integration of regenerated cells with the surrounding tissue, enabling seamless healing and minimizing the risk of complications.[14,15] While BNCs hold immense potential for skin tissue repair and regeneration, several challenges need to be overcome. Addressing issues of biocompatibility, mechanical properties, degradation rate, biomimicry, scalability, stability, regulatory approval, and clinical translation are essential for the successful application of BNCs in this field. Developing scalable and cost-effective manufacturing methods for BNCs is a significant hurdle. Ensuring consistent quality, reproducibility, and scale-up production of BNCs is necessary for their widespread use in skin tissue repair and regeneration. Notably, bridging the gap between laboratory research and clinical implementation is essential. In this context, conducting rigorous preclinical and clinical studies, addressing ethical considerations, and ensuring affordability are crucial for successful clinical translation.

Herein, this review aims to provide a comprehensive overview of the current trends, advantages, challenges, and future directions in the field of BNCs for skin tissue repair and regeneration. By consolidating existing knowledge and highlighting advancements made in the development and application of these BNCs, this review seeks to shed light on their potential in promoting skin tissue repair. It explores the different types of BNCs and the unique properties that make them advantageous for tissue regeneration. In addition, the review addresses the challenges faced in terms of biocompatibility, mechanical properties, and regulatory approval, while also focusing on potential future directions and emerging research areas. While there have been previous reviews on this topic, this review presents the latest research findings, emerging trends, and recent advancements in the field. Furthermore, it highlights the potential future directions and identifies research gaps that need to be addressed to further advance the field. By providing a fresh perspective and incorporating the latest research, this review offers a novel contribution to the existing body of knowledge on BNCs for skin tissue repair and regeneration.

2. Wound repair and regeneration: mechanisms, signaling, and translation

After an injury, rapid wound closure and regeneration of the damaged skin are crucial for restoring its protective function. Wound healing is a complex but finely-tuned process that begins immediately after an injury and can continue for months or even years.[28] Effective wound repair is precisely orchestrated and regulated at multiple levels and requires communication and interaction between various cell types. The wound healing process can be broadly categorized into four sequential but overlapping phases: hemostasis, inflammation, proliferation, and remodeling.[29] Deregulation of any of these phases leads to impaired healing, such as the development of chronic, difficult-to-heal ulcers, or excessive scarring (Fig. 2 (A)).[5]

2.1. Hemostasis

Immediately after an injury, the damaged endothelium releases endothelin-1, which leads to vasoconstriction.[31] In addition, the contact of platelets with the exposed components of the sub-endothelial vascular matrix, *e.g.* collagen, results in platelet activation.[32] The primary aim of these rapid responses is to prevent blood loss and to initiate the early phases of the coagulation process. Platelets adhere *via* receptors such as glycoprotein VI (GPVI) and integrin $\alpha_2\beta_1$ to proteins of the ECM, especially to collagen of the injured blood vessel wall.[33] In addition, the plasma von Willebrand Factor (vWF) binds to the exposed collagen, which undergoes a shear-induced conformational change. The immobilized vWF then initiates the adhesion of platelets *via* binding to glycoprotein (GP)Ib-IX

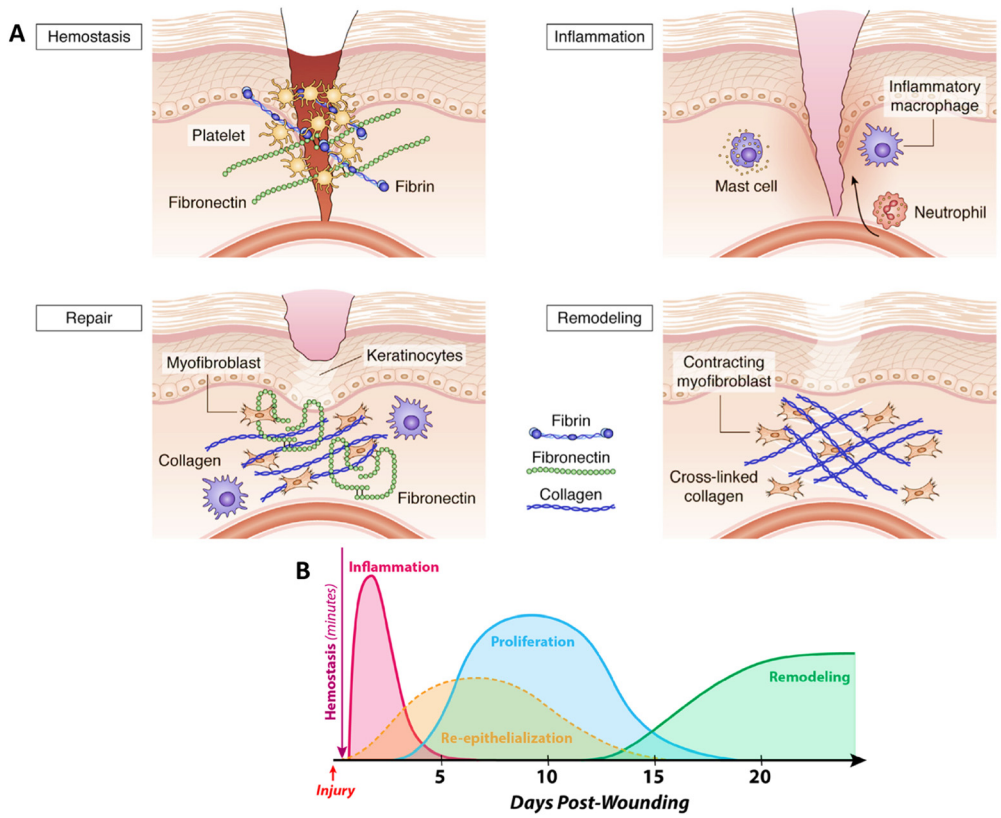

Fig. 2 Mechanisms of wound healing: (A) different phases of wound healing. Reprinted from[5] under the terms of the Creative Commons Attribution License (CC BY). (B) Timeline of cutaneous wound healing. Reprinted from[30] under the terms of CC BY license.

complex (CD42) on the platelets[34] followed by triggering the platelet activation by thrombin that leads to a conformational change, and the release of alpha and dense granules containing cytokines and growth factors (like platelet-derived growth factor (PDGF), transforming growth factor beta (TGF-β), basic fibroblast growth factor (bFGF), insulin-like growth factor-1 (IGF-1), and vascular endothelial growth factor (VEGF)) along with coagulation factors that promote coagulation and platelet aggregation.[35]

This process concludes with the formation of an insoluble clot known as the eschar, which is composed of platelets, fibrin, fibronectin, vitronectin, and thrombospondin,[36] and effectively seals the wound, prevents further bleeding, and serves as a provisional matrix. Beyond its hemostatic role, the eschar also prevents bacterial invasion, serves as a scaffold for cell migration, and as a reservoir for cytokines and growth factors released by activated platelets to guide the behavior of wound cells during the early stages of repair.[37] The released cytokines attract circulating inflammatory cells to the side of the wound, trigger tissue movements for re-epithelialization and connective tissue contraction, and stimulate the angiogenic response of the wound.

2.2. Inflammation

The second phase of wound healing is the inflammatory phase, which begins immediately after hemostasis and lasts around 4–6 days (Fig. 2(B)).[30] This phase can be divided into two separate phases, the early inflammatory phase and the late inflammatory phase.[38]

Early inflammatory phase. Following injury, resident skin cells, including mast cells, keratinocytes, Langerhans cells, and dendritic cells, are exposed to danger signals including damage-associated molecular patterns (DAMPs), released by necrotic cells and damaged tissue,[39] and pathogen-associated molecular patterns (PAMPs) originating from bacterial compounds. These DAMPs and PAMPs activate resident immune cells such as mast cells and Langerhans cells by binding to pattern recognition receptors (PRRs), triggering downstream inflammatory pathways.

Upon activation, mast cells release granules containing enzymes, notably histamine, resulting in vasodilation and increasing vascular permeability.[40] In addition, the release of pro-inflammatory cytokines and chemokines induces the expression of endothelial adhesion molecules, such as intercellular adhesion molecule 1 (ICAM-1), vascular cell adhesion molecule 1 (VCAM-1), P- and E-selectin, on the surface of blood vessels.[41] This, in turn, enables the adhesion of circulating neutrophils and monocytes to the inflamed endothelium and promotes their extravasation into the affected tissue. Previous studies in which E- and P-selectin were blocked led to a significant impairment of immune cell infiltration and wound healing process and demonstrated the significance of selectins for the recruitment of immune cells.[42,43]

Neutrophils are recruited by chemoattractants, such as leukotriene B4 or LTB4, the chemokines (C-X-C motif) ligand-5 (CXCL5) and CXCL8, the complement anaphylatoxins C3a and C5a, and the bacteria-derived formly peptides *N*-formyl-Met-Leu-Phe (fMLF), into the wound site.[44] In response to pro-inflammatory signals, neutrophils, along with other cells present at the wound site, release cytokines such as interleukin 1β (IL-1β), IL-6, and tumor necrosis factor-alpha (TNF-α).[45] This initiates the activation of inflammatory signaling pathways, such as nuclear factor kappa B (NF-κB), which in turn, further recruits and activates fibroblasts and epithelial cells in the wound healing process.[46] Furthermore, the neutrophils recruited to the wound site play a crucial role in the elimination of damaged cells and pathogens by various mechanisms, like phagocytosis.[47] These cells also deploy an array of weapons, such as the release of reactive oxygen species (ROSs), antimicrobial peptides, eicosanoids, and proteases *e.g.* neutrophil elastase and collagenase.[37] These proteases remove components of the ECM damaged by the initial injury. In addition, neutrophils trap and kill pathogens in an extruded web of DNA–histone complexes coated with antimicrobial peptides and proteins released by activated neutrophils, known as neutrophil extracellular traps (NETs).[48,49] Typically, the presence of neutrophils in the wound diminishes after 2 to 3 days due to the process of apoptosis, and they are subsequently replaced by attracted monocytes into the tissue.[35] Apoptotic neutrophils are removed by tissue-resident macrophages *via* efferocytosis.[50]

Late inflammatory phase. Approximately 24 h post-injury, monocytes are recruited to the site of injury, where they undergo differentiation into macrophages.[35] Macrophages play a fundamental role in late stages of inflammation and typically appear 48–72 h after the initial injury. They remove devitalized tissue by releasing matrix metalloproteinases (MMPs) and elastase and engulfing necrotic cellular debris and pathogenic material. Moreover, they orchestrate the process of wound healing by transitioning from predominantly pro-inflammatory (M1-like phenotype) to the anti-inflammatory (M2-like phenotype),[51] which is crucial for modulating the transition from the inflammatory phase to the proliferative phase of healing. Macrophages also release a variety of growth factors and cytokines, including IL-6, TNFα, IGF-1, TGF-β, TGF-α, FGF, and IL-1, which can activate fibroblasts, endothelial cells, and keratinocytes.[35] Thus, macrophages play pivotal roles in modulation of skin repair and wound closure. Since macrophages are among the main producers of inflammatory cytokines, their depletion during wound healing also leads to reduced scar formation, indicating their involvement in fibrosis.[52]

2.4. Proliferation

The proliferation phase starts 3 days after the injury and lasts about 2 weeks.[38] During this phase, the provisional fibrin matrix is replaced by a new matrix of collagen fibers, enriched in proteoglycans, and fibronectin, to restore the structure and function of the tissue.[53] Crucial events in this phase include the formation of granulation tissue, re-epithelialization, and angiogenesis to replace previously damaged vessels and restore circulation.

Migration of fibroblasts and collagen synthesis. Fibroblasts migrate into the wound in response to cytokines and growth

factors such as PDGF, TGF-β, and bFGF, which are initially released by platelets and later by macrophages within the wounds.[54] To facilitate their movement through the tissue matrix, fibroblasts locally secrete proteolytic enzymes. On the third day post-injury, fibroblasts appear in the wound, where they proliferate and release proteinases like MMPs to degrade the provisional matrix. Simultaneously, fibroblasts deposit collagen along with other ECM components, such as hyaluronic acid, fibronectin, and glycosaminoglycans.[29] This process leads to the replacement of the provisional matrix by granulation tissue, characterized by a large number of fibroblasts, macrophages, blood vessels and capillaries, and loosely organized collagen fibers.[5] By the end of the first week, a substantial accumulation of ECM occurs, filling the wound gap, and providing a scaffold that facilitates cell adhesion, migration, growth, and differentiation during the wound repair process. Fibroblasts undergo a transition to the myofibroblast phenotype, characterized by the presence of thick actin bundles beneath the plasma membrane and the expression of α-smooth muscle (SM) actin. These cells exhibit contractile properties, attributed to the α-SM actin expression in microfilament bundles or stress fibers, playing a pivotal role in the contraction and maturation of the granulation tissue.[55] Wound contraction, which is achieved through the retraction of cell extensions, helps to approximate the wound edges. Once this task has been accomplished, redundant fibroblasts are eliminated by apoptosis, contributing to the refinement and resolution of the healing process.[56]

Angiogenesis. To replace damaged vasculature and maintain tissue viability, angiogenesis is induced by local microenvironment factors, including low oxygen tension, low pH, and elevated lactate levels.[57] In addition, keratinocytes, fibroblasts, vascular endothelial cells, and macrophages produce angiogenic factors, such as bFGF, TGF-α, TGF-β, and VEGF, which are potent angiogenic signals for endothelial cells.[58] Furthermore, oxygen levels in tissues directly regulate angiogenesis by interacting with oxygen-sensing proteins that could affect transcription of angiogenic and anti-angiogenic genes.[59] For instance, hypoxia stimulates the synthesis of VEGF by capillary endothelial cells *via* the activation of the transcription factor, hypoxia-inducible factor (HIF).[60] As the oxygen levels surrounding capillary endothelial cells decrease, intracellular HIF levels increase, which then binds to hypoxia response elements (HREs) and stimulates transcription of specific genes such as VEGF that facilitate angiogenesis.[61]

Epithelialization. The migration of epithelial cells, specifically keratinocytes, starts from the wound edges within a few hours to one day of wounding.[62] Growth factors released during the healing process, such as epidermal growth factor (EGF), keratinocyte growth factor (KGF), and TGF-α, stimulate the migration and proliferation of keratinocytes at the basal layer of the wound edge to cover the wound.[63] The migration process is triggered by the loss of contact inhibition and physical tension at cell adhesion structures, namely desmosomes and hemidesmosomes, which activate membrane-associated kinases, resulting in increased membrane permeability for calcium – an essential signal for cytoskeleton reorganization that drives migration.[29] Subsequently, integrin receptors are expressed, causing the typically cuboidal basal epithelial cells to flatten and migrate as a monolayer over the newly formed granulation tissue, following along collagen fibers.[64] During migration, these cells secrete proteolytic enzymes (MMPs) to penetrate through the eschar. Migration stops when the cells come in contact and new adhesion structures are formed. The entire epithelial layer enters a proliferative mode, and the stratified layers of the epidermis are re-established and begin to mature to restore the barrier function.

2.5. Remodeling phase

The final phase of the healing process is the remodeling phase, which begins two to three weeks after the injury and can last one year or longer.[65] During the remodeling phase, the granulation tissue matures into a scar, and the tensile strength of the tissue is increased.[66] This maturation process is accompanied by a decrease in the number of capillaries *via* aggregation into larger vessels. In addition, the cell density and metabolic activity in the granulation tissue are reduced. The initially produced type III collagen in the ECM is replaced by type I collagen,[67] which is the dominant fibrillar collagen in the skin and has a higher tensile strength. This replacement is regulated by MMPs.[68] Over several months or longer, alterations in collagen organization within the repaired tissue slowly increase the tensile strength to a maximum of about 80% of normal tissue.[69]

3. BNCs in skin tissue engineering and regenerative medicine

One of the areas that tissue engineering and regenerative medicine focuses on is creation as well as regeneration of tissues and organs. For this purpose, use of biopolymers has attracted attention due to their significant advantages over synthetic polymers. They are biocompatible, biodegradable, could have additional functionalities based on the biopolymer, and perform well in applications due to hydrophilic characteristics.[16] Their benefits encompass the replication of natural pathways for tissue regeneration, and restoration of physiological functions. Some biopolymers, such like collagen, are inherent to the ECM structure, and some could participate in natural healing mechanisms by supporting cell migration, adhesion, proliferation, and cell differentiation, and directing cell alignment. Moreover, some biopolymers have important intrinsic properties like antimicrobial, hemostatic, anti-inflammatory properties that further support the material properties.[16,70–72]

Nanomaterials could improve the solubility of drugs, reduce doses, enable targeting, minimize toxicity, and enhance bioavailability. They include a diverse class of materials with different compositions such like metallic NPs, engineered therapeutic agents like oligonucleotides, or nano-sized polymeric structures.[73] Developments in nanotechnology in the last

decades also have paved the way for new approaches in tissue engineering; there is a significant focus on nanotechnology within the realm of biopolymer matrix-based BNCs across diverse applications. BNC materials has been a subject that has been studied extensively in recent years.[74] By expanding the scope of biocomposites to include nanostructured hybrid materials, the term 'bionanocomposites' can be defined in two distinct ways. Firstly, it can refer to nanocomposites crafted from renewable NPs in conjunction with petroleum-derived polymers. Secondly, BNCs is defined as nanocomposites derived from biopolymers paired with synthetic or inorganic nanofillers. Nano-elements in BNCs could support skin repair mainly either by unique properties of the particles or by encapsulation of functional elements that promote cellular growth and repair.[75] NPs could be added to the BCS by different methods. A method is *in situ* formation of NPs within the polymer matrix. An example of this method is chemical reduction of silver ions and formation of Ag-NPs *in situ*. In *ex situ* procedure, NPs are prepared and later added to the polymer matrix.[76,77] Surface modification is another approach in preparation of the functional dressings. In a study, Harandi *et al.* make surface modification of wound dressing material NPs incorporating *Lactobacillus* strains. In the study two hybrids *Lactobacillus plantarum* and *Lactobacillus acidophilus*-green Fe_2O_3 NPs were used for surface-coating of electrospun wound dressing enhanced antimicrobial and antibiofilm activity.[78]

Creation of a moisty environment is an important aspect of wound healing to support healing. However, overhydration could cause delayed healing and may cause undesired effects such like maceration that could lead softening and breaking down of the surrounding skin as well as infections.[79] Also, addition of NPs could be useful in surface hydrophilic/hydrophobic regulation. Some studies suggest that addition of NPs to films changed water vapor permeability (WVP) of the films. Generally, a decrease in WVP was observed in compatible polymers, while an increase is observed in nanoclusters due to increased water diffusion through the dressing, or loose packaging of hydrophilic and hydrophobic components within the NC that allows WVP.[80,81] In this part, BNCs in skin tissue engineering and regenerative medicine is discussed, and the recent studies in this field have been reviewed.

3.1. Natural polymers

3.1.1. Silk fibroin-based BNCs. Silk fibroin (SF) is a Food and Drug Administration (FDA)-approved natural protein with notable regenerative properties. SF boasts exceptional mechanical strength, water vapor and oxygen permeability, biocompatibility, biodegradability, and low immunogenicity, leading to its extensive use in tissue engineering. In addition, SF serves as a biomaterial for wound and skin damage repair due to its minimal inflammatory reaction, hemostatic abilities, and permeability to oxygen and water vapor.[82,83] It also supports well the human keratinocytes and fibroblasts.[84] In the case of skin wound healing, SF advances the process through the NF-kB signaling pathway, which governs essential cellular properties such as inflammation, adhesion, proliferation, and the elimination of reactive oxygen species.[85]

SF nanofibrous scaffolds, a compelling type of SF-derived skin substitute, are created using electrospinning to establish a pseudo 3D network for optimal cell adhesion and growth.[85] The pores formed between the nanofibers not only facilitate oxygen exchange but also effectively prevent the infiltration of external fluids and bacteria. This unique combination of properties creates an ideal microenvironment for promoting cell proliferation and skin regeneration.[86] Sheikh *et al.* identified 3D SF nanofiber scaffolds as an excellent choice for artificial skin reconstruction, emphasizing their potential for scarless regeneration of fetal skin.[87] In another study by Wang *et al.*, a silk-based construct incorporating hyaluronic acid (HA), SF, and silk nanofiber was developed to mimic the ECM and improve the healing process. The introduction of HA resulted in remarkable water-binding potential, high-porosity, and mechanical stability. The incorporation of silk nanofibers demonstrated a benefical impact on hindering scar formation. This innovative avenue, leveraging an ECM-like SF scaffold, holds great potential for biomaterial configuration and applications in skin tissue engineering.[88] In another study, Du *et al.*, created a nanofiber composite of SF–gelatin enriched with propolis, demonstrating favorable physical properties. They incorporated varying amounts of propolis into the nanofiber to enhance its healing and antibacterial capabilities. The findings revealed that the inclusion of propolis caused changes in the physicochemical features of SF–gelatin nanofibers, resulting in a significant enhancement of their antimicrobial features and effective promotion of healing. The nanofibers containing SF–gelatin–propolis extract show considerable promise for applications in skin tissue engineering and wound treatment.[21] In another study, Gao *et al.*, employed electrospinning to create a periplaneta americana extract-implemented SF nanofiber mat. This mat displayed a considerably higher wound closure rate in the mouse model of full-thickness wounds compared to commercial products. Histomorphological assessments revealed that the periplaneta americana extract-implemented SF nanofiber mat promoted re-epithelialization, angiogenesis, and collagen deposition at wound sites, facilitating the overall wound healing process.[89]

Double-layered wound dressings with multifunctional features can be appealing for efficient skin regeneration. Farshi *et al.*, innovatively designed a double-layered wound dressing, combining electrospun SF for enhanced mechanical strength in the upper layer and a carboxymethyl cellulose (CMC)/gelatin composite film as the skin-interacting substrate. In wound dressing applications, CMC exhibits limited mechanical stability and low cellular activity. To address these shortcomings, a suggested approach involves combining CMC with SF to create a more effective dressing. The mechanical properties of the resulting double-layered wound dressing significantly improved with the incorporation of SF. In addition, the dressing promotes increased cell proliferation, attributed to the cytocompatible characteristics of SF. Consequently, results showed the capacity of this developed structure as an encouraging choice for skin

tissue regeneration.[90] In another work, Liu *et al.*, created SF sponges with nanopore-containing walls derived from SF NPs produced during autoclaving of SF solutions (Fig. 3(A)). These nanopores proved beneficial for wound healing by improving exudate absorption, maintaining moisture, facilitating nutrient and gas diffusion, and enhancing cell adhesion (Fig. 3(B)). In a rat skin wound model, SF sponges with nanopores exhibited superior performance in speeding up wound healing, promoted by increased collagen accumulation (Fig. 3(D)), vascularization, and epidermal thickness (Fig. 3(C)) over 21 days, compared to samples without nanopores. This biomaterial, featuring a hierarchical multi-scale pore shape, offers a novel strategy for designing and engineering high-performing skin tissue constructs that can independently support vascularization, cell migration, and tissue regeneration without the addition of growth factors.[22]

3.1.2. Hyaluronic acid-based BNCs. Hyaluronic acid (HA) is a linear disaccharide polymer of ECM that could be found abundantly in the connective tissue and has essential functions in some main steps of wound healing including cellular growth and differentiation as well as contributing in initial inflammation.[2,91] Furthermore, various cell membrane receptors, including receptor for Hyaluronan Mediated Motility (RHAMM), CD44, and ICAM-1 have been demonstrated to interact with HA influencing biological activities such as cellular growth, angiogenesis, migration, and wound healing.[92] HA also possesses the ability to sustain skin hydration and enhance both permeability and viscoelasticity.[93]

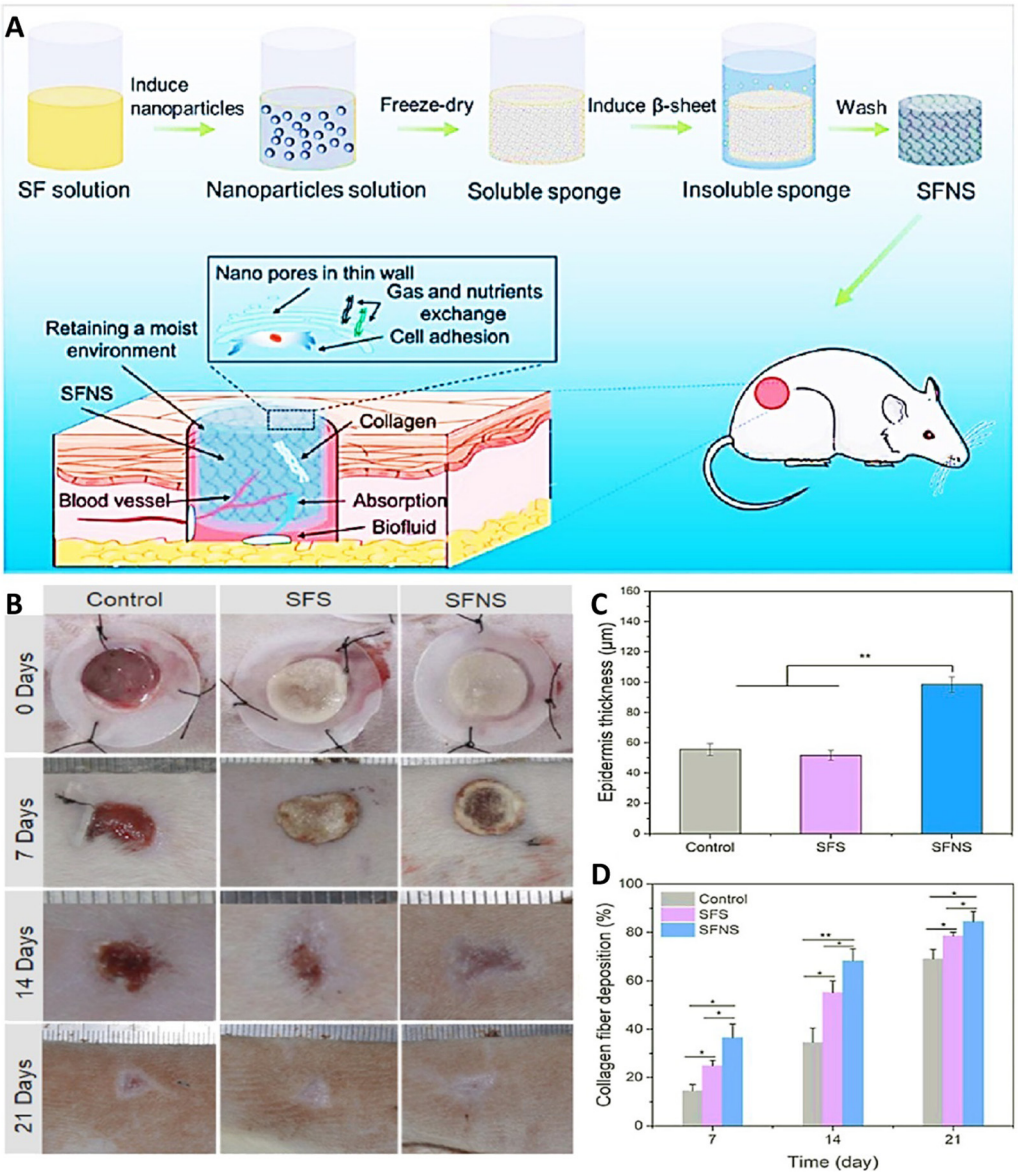

Fig. 3 (A) Schematic of SF sponges with nanopore-containing walls derived from SF NPs supporting wound repair through a number of mechanisms. (B) Image of wound healing results for 21 days. Results of thickness of the epidermis (C) and collagen accumulation (D) after exposing with different treatment (*$p < 0.05$, **$p < 0.01$). Reprinted with permission from.[22] Copyright 2023, American Chemical Society.

The limited clinical applications of HA-based scaffolds are often attributed to their poor mechanical properties. To overcome this challenge, the implementation of supporting elements such as nanocrystalline cellulose (CNC) into HA-based wound dressings has shown promise in improving mechanical properties. Furthermore, enhancing the healing process can be achieved through the controlled delivery of growth factors to the wound area using NPs. In research done by Dehkordi *et al.*, a new wound dressing was developed, consisting of CNC-reinforced HA-based nanocomposites. This innovative dressing also incorporated chitosan NPs loaded with granulocyte macrophage colony stimulating factor proteins (GM-CSF). Chitosan NPs loaded with GM-CSF were synthesized using the ionic gelation method, resulting in particles with a size of about 366.9 ± 9.15 nm. The controlled release of GM-CSF over a 48-h period from the composite wound dressings was achieved, offering a more favorable healing environment compared to the rapid release of this growth factor. Wound dressings incorporating GM-CSF-loaded chitosan NPs demonstrated superior effects on wound healing when compared to pristine dressings (completely healed the wound in 13 days in rats treated with CNC-HA/GM-CSF-Chi-NPs composite, while in control cases 70% wound size reduction was seen). Release of GM-CSF in the structure of this dressing led to reducing the inflammation, enhancing the granulation tissue formation, and accelerating re-epithelization as compared with hydrogels without it.[94]

Li *et al.*, developed a HA BNC using aldehyde-functionalized sodium hyaluronate, hydrazide-functionalized sodium hyaluronate, and aldehyde-functionalized cellulose nanocrystals (oxi-CNC). Platelet-rich plasma (PRP) was implemented into the HA nanocomposite constructs to synergistically support skin wound healing. The fabricated formulation provided the capability of sustained release of PRP from the hydrogel, resulted from the interactions between hydrogel network and PRP, that enhanced the therapeutic effects of growth factors incorporated inside PRP on the wound site. In animal experiments, the PRP-loaded HA nanocomposite hydrogels significantly enhanced full-thickness skin wound healing by promoting tissue granulation (1147.43 ± 31.07 μm), simplifying collagen accumulation (63.93 ± 1.45%), and ascending neovascularization and re-epithelialization. It showed accelerated wound closer (95.28 ± 0.56%) compared to rats exposed with the only gel (92.05 ± 2.13%) and the control group (90.29 ± 1.68%).[95] Hu *et al.* (2022) addressed the challenge of abdominal wall injuries, often complicated by serious infections, by developing a multifunctional hydrogel.[96] This construct on the basis of dopamine-functionalized HA, gelatin, and AgNPs, aimed to advance the repair of abdominal wall damages. In rat full-thickness skin injury model and rat full-thickness abdominal wall injury model, the developed construct demonstrated the ability to speed up the healing function. It achieved this by decreasing wound inflammation, enhancing wet adhesion, and supporting the generation of granulation tissues and angiogenesis. The developed system exhibited great potential for the full-thickness abdominal wall defect therapy.[96]

A versatile wound dressing was created by incorporating graphene oxide/copper nanocomposites with HA/chitosan constructs. This innovative approach represents an encouraging choice for successful therapeutic intervention in bacteria-infected wound healing, especially in the context of plastic surgery clinics. The fabricated formulation showed a sustainable pH responsive release behavior so that the amounts of released copper NPs were increased by decreasing pH (about 60.3%, 76.2% and 88.1% under alkaline, neutral, and acidic conditions, respectively, after 14 days). Presence of Cu and its release from this formulation provided high bactericidal and antibiofilm abilities for the hydrogel and confirmed its effectiveness in treatment of infected wound. The developed multifunctional constructs significantly accelerated wound healing (wound closer area of about 93.1 ± 1.2%, 61.7 ± 3.7%, 39.2 ± 8.0%, and 18.5 ± 2.1% for the C/H/GO/Cu, C/H/GO, C/H, and control groups, respectively), featuring regulated inflammatory infiltration, and enhanced angiogenesis in granulation tissues. Besides, there was no bacterial infection in cases treated with the C/H/GO, C/H scaffold that could be due to the presence of GO/Cu nanocomposites, along with the CuNPs, and Cu^{2+} released from the dressing scaffolds throughout the wound healing process. Importantly, no pathological injury was observed in the tissue constructs of examined organs, including the liver, lung, kidney and heart.[97] Zhou *et al.* (2021) created a 3D printing platform to mimic full-thickness skin by mixing catechol–hyaluronic acid (HACA) with sodium alginate and calcium chloride, and gelatin with horseradish peroxidase and hydrogen peroxide.[98] The developed bioink was first printed using 3D-printing method and then thrombin-free fibrinogen, combined with human dermal fibroblasts, was applied to induce the gelation of bio-printed scaffolds. After removing the gelatin, human HaCaTs keratinocytes were placed on the printed scaffold to grow and generate skin-like networks. The printed-construct, demonstrated high elasticity, promoted the creation of a double-layered, and cell-laden skin-like network. The findings indicate that this 3D printing system establishes a groundwork for skin regeneration.[98]

Chang *et al.* (2023) engineered an enzyme-crosslinked HA–tyramine based hydrogel wound dressing that incorporates antioxidants and photothermal AgNPs (HTA) (Fig. 4). AgNPs capped with natural antioxidant tannic acids were synthesized, utilizing tannic acids as stabilizing and reducing agents in the process.[99] The NPs had a size of 149 nm, a zeta potential of 26.4 mV, and a polydispersity index (PDI) of 0.24, indicating their relative stability. Encapsulation of AgNPs capped with TA significantly enhanced the hydroxylic radical scavenging ability due to the presence of TA, a natural polyphenol small molecule. Moreover, these TA could interact with metal ions and concentrated Ca^{2+} (coagulation factor IV) that led to an enhanced hemostatic performance. Utilizing near infrared (NIR) light led to a stable photothermal effect dependent on the concentration of AgNPs@TA. This photothermal ability was used to improve the antibacterial activity of hydrogel so that by increasing the time of NIR irradiation from 1 to 3 min, the amounts of bacterial colony reached to zero (Fig. 4(A)). Besides, utilizing

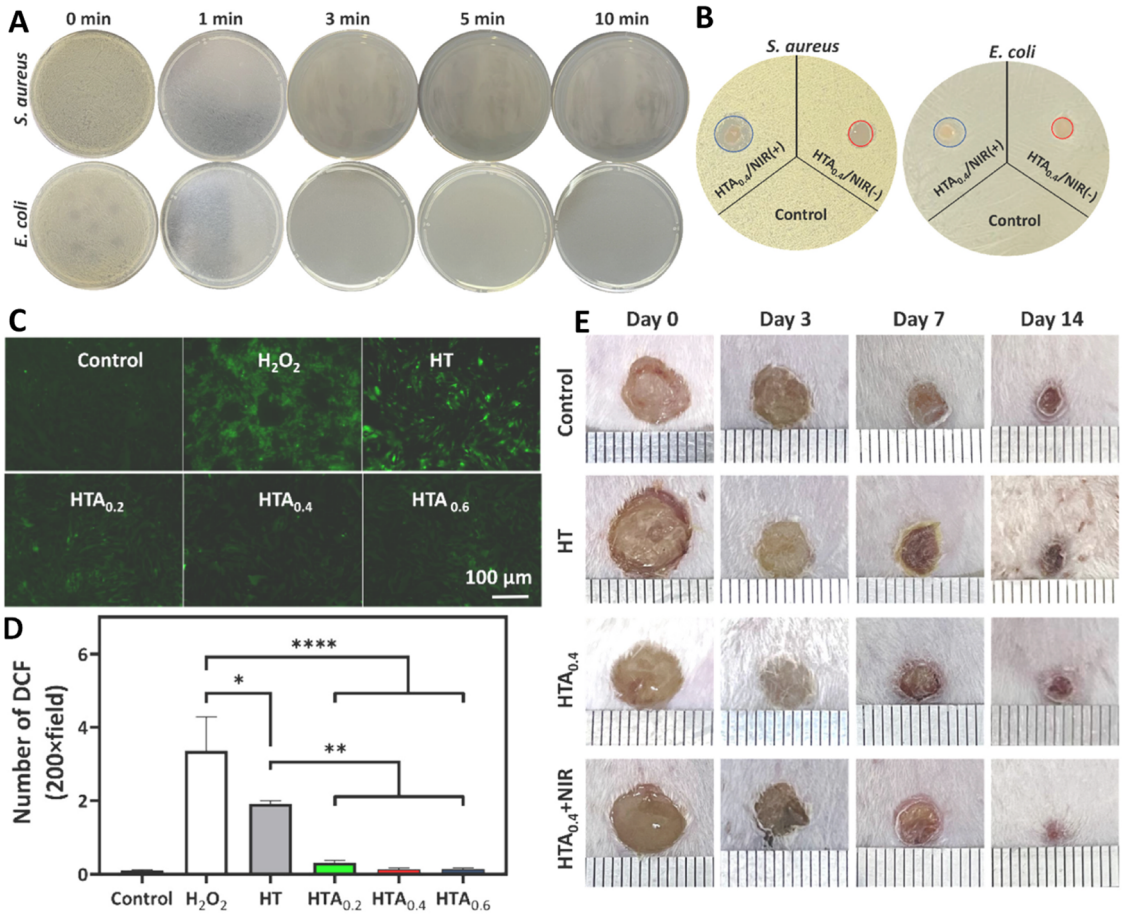

Fig. 4 Antibacterial activity against *S. aureus* and *E. coli* using (A) clony counting assay after 0, 1, 3, 5, 10 min exposing with near infrared (NIR) light and hyaluronic acid–tyramine (HT) loaded AgNPs (HTA) hydrogel, and (B) inhibition zone assay in the presence of HTA with/without NIR. (C) and (D) The antioxidant results of different samples (control, H_2O_2, HT, HT + 0.4 mg ml^{-1} of AgNPs@TA ($HTA_{0.4}$), and $HTA_{0.6}$) using qualitative and quantitative methods. (E) Wound healing results of mice model after exposing with different treatments. Reprinted with permission from.[99] Copyright 2022, Elsevier.

NIR led to expanding the inhibition zone of $HTA_{0.4}$ hydrogel against both Gram-positive and Gram-negative bacteria (Fig. 4(B)). Presence of AgNPs@TA in the structure of this hydrogel induced antioxidant activity in it so that cells treated with hydrogels contained NPs had high antioxidant activity (Fig. 4(C) and (D)). The combination use of NIR and $HTA_{0.4}$ hydrogel accelerated the healing ratio of wound in animal model (Fig. 4(E)) *via* improving collagen deposition, re-epithelilization, and tissue regeneration.[99]

3.1.3. Collagen-based BNCs. Collagen, the most prevalent protein in mammals, serves as the primary element of the ECM, contributing to the elasticity and strength of the skin.[100] Widely utilized in skin tissue engineering, collagen stands out because of its natural abundance, biocompatibility, minimal immunogenic response, biodegradability, and good permeability. Collagen is effective in accelerating wound healing by reinforcing a proper environment for the proliferation keratinocyte and fibroblast.[101] Collagen plays a vital role in the tissue-remodeling phase *via* controlling tissue structure and repairing strength of injured skin, as well as promoting the rapid angiogenesis.[102,103] However, it has weak mechanical and physical behaviors that makes it important to use it in combination with other materials that could improve their properties.[104] In a research paper by Sharifi *et al.* (2023), a biocompatible collagen-based skin substitute was developed for skin regeneration in full-thickness non-pathological wounds.[104] Zinc-doped bioactive glass–ceramic (Zn-BGC) was incorporated to enhance angiogenesis and wound healing behaviors (Fig. 5). The resulting col–gel/Zn-BGC BNC porous hydrogel demonstrated biocompatibility and supplied an appropriate 3D microenvironment for cell proliferation and adhesion. When loaded with mouse embryonic fibroblasts, this hydrogel scaffold increased wound healing and supported skin appendage regeneration in mice with excisional full-thickness wounds.[104] In another study by Kalirajan *et al.*, a collagen-based hydrogel scaffold bioengineered with a silver–catechin nanocomposite was fabricated for scarless healing of infected diabetic burn wounds. An oxidized jackfruit seed polysaccharide served as a crosslinking element to stabilize the collagen scaffold. *In vivo* experiments were conducted using BNC hydrogel scaffold on diabetic and non-diabetic rats with chronic burn wounds. Notably, the BNC hydrogel scaffold showed better healing in contrast to pristine collagen scaffold. Herein, the epidermal thickness in diabetic animals treated with the BNC hybrid scaffold reduced to 33 ± 2 μm, compared to 90 ± 2 μm in

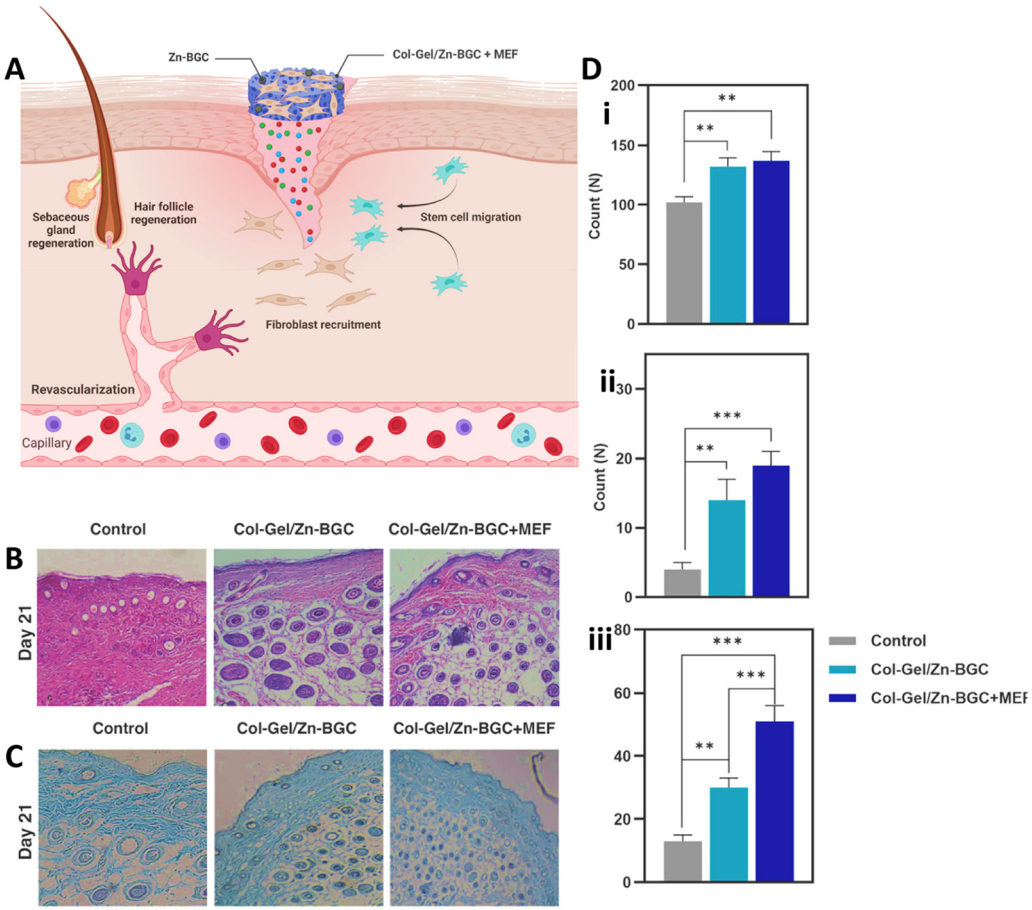

Fig. 5 (A) Supportive function of collagen–gelatin/Zn-BGC BNC construct encapsulated with mouse embryonic fibroblasts for cutaneous wound healing by promoting revascularization, regenerating hair follicles, recruiting fibroblasts, and facilitating re-epithelialization. (B) Hematoxylin–eosin (H&E) staining on day 21. (C) Masson's Trichrome staining on day 21. (D) Quantification of fibroblasts (i), blood vessels (ii), and hair follicles (iii) in skin wounds for both the control and test groups on day 21. (Statistically significant at **: $p < 0.01$, ***: $p < 0.001$). Reprinted with permission from.[104] Copyright 2023, Elsevier.

those treated with the pristine collagen scaffold. The scar elevation index (SEI) value of the pristine collagen scaffold treated diabetic and non-diabetic rats was found to be 2.1 ± 0.1 and 1.8 ± 0, respectively. In contrast, SEI value of BNC scaffolds was detected to be 1.3 ± 0.1 and 1.2 ± 0.1 for diabetic and non-diabetic rats, respectively. This means that the BNC hydrogel scaffold, when applied to diabetic animals, resulted in SEI of 1.3 ± 0.1, closely resembling normal skin. The findings indicated that animals treated with the BNC hydrogel scaffold displayed reduced levels of TGF-β1 expression and elevated levels of TGF-β3 which were crucial in promoting a wound healing environment that is favorable for scarless recovery.[105]

ZnO–curcumin implemented collagen BNC was fabricated for efficient scarless skin regeneration in acute burn injuries. The ZnO–curcumin nanocomposite in the hybrid structure up-regulated angiogenesis and TGF-β3 expression thereby reduced the scar formation. It was shown that the native collagen had antioxidant activity which was significantly improved by the addition of ZnO–curcumin nanocomposite. The hybrid of ZnO and curcumin also led to decreasing the inflammatory effect *via* down-regulating the expression of tumor necrosis factor-α (TNF-α) and interleukin-1 (IL-1). Evaluation of the newly regenerated epidermis thickness and relative scar elevation index (SEI) value in animals treated with the hybrid construct indicated scarless wound healing. Curcumin could also accelerate proliferative stage *via* improving the proliferation and migration of fibroblasts. On the other hand, Zn^{2+} ions enhanced the migration of keratinocytes *via* acting as cofactor for enzymes like zinc dependent matrix metalloproteinases. All of these led to improved wound healing effect that was confirmed by enhancing collagen deposition, neovascularization, and re-epithelialization. Results showed wound closer percentage of about 82 and 91% for collagen–ZnO (Coll/OTSP/ZnO 5%) and collagen–curcumin (Coll/OTSP/Cur 5%) scaffold compared to 65 and 80% for untreated and native collagen scaffold.[106] In another work, Khadivar *et al.* fabricated a biocompatible collagen-based nanoscaffold using collagen, carboxymethylated diethyl aminoethyl cellulose, and wood nanocellulose for skin tissue engineering applications. *In vitro* studies conducted on MSCs and keratinocytes demonstrated the biocompatibility of the nanocomposite scaffold. *In vivo* studies were carried out to assess potential immunogenic or allergic behaviors of the

nanocomposite scaffold. Transforming growth factor β (TGF-β), a multifunctional cytokine associated with inflammation, was screened on day 3 to evaluate any immune reaction triggered by the scaffold. The lower level of TGF-β expression in wounds treated with scaffold proved that the nanocomposite scaffold did not induce significant allergic or immune reactions. On day 21 of treatment, cytokeratin 18 (CK18) and collagen deposition were examined to assess the extent of skin reconstruction. The developed nanocomposite scaffold facilitated the wound regeneration process and accelerated overall healing. The scaffold, with its moisture-absorbing capability, support for cell adhesion, high zeta potential, and satisfactory stability properties, emerged as a potent film for wound healing and skin tissue engineering.[107]

Collagen nanofibers were developed through electrospinning, incorporating nanophase hydroxyapatite crystals for the purpose of skin regeneration and repair. The release of calcium ions from the nano-hydroxyapatite improved cellular growth and proliferation rates, while preventing the pathogenic bacteria adhesion appeared in human skin flora. Implantation of the collagen/nano-hydroxyapatite BNC in rat subcutaneous tissue demonstrated the absence of adverse reactions. Consequently, this mechanically robust composite membrane holds significant potential for utilization either as a scaffold for cell transplantation in skin wound regeneration or as a wound dressing biomaterial in applications such as burn therapy, plastic surgery, or addressing various skin diseases.[108]

The development of multifunctional hydrogel adhesives that can inhibit infections and enable electrical stimulation for tissue repair is extremely desired for healing surgical wounds and other skin damages.[109] In a recent work, Gu *et al.* developed a collagen-based self-healing and injectable hydrogel composed of collagen/chitosan/oxidation-modified Konjac glucomannan hydrogel matrix (COL–CS–OKGM) with multifunctional capabilities for the regeneration of infected wounds. OKGM was used as crosslinker to build dynamic Schiff-base bonds. Collagen and chitosan were chosen for their strong synergistic compatibility, aiming to create a complex that mimics the composition of the ECM. The integration of AgNPs into the hydrogel resulted in significantly enhanced antibacterial activity stemmed from the synergistic effect between the released Ag^+ ions and the mild photothermal potential of AgNPs. Indeed, utilizing NIR irradiation enhanced the release of Ag^+ ions which were then interacting with the sulfhydryl groups on the surface of bacteria, destroying their membrane, affecting the nucleic acid of bacteria that led to bacterial death. It also enhanced local capillary blood circulation in the wound site and facilitated the wound healing procedure. The COL–CS–OKGM hydrogel, with self-healing behaviors, facilitates the dressing to conform seamlessly to irregular wound surfaces, establishing an optimal moist environment for the healing process. The COL–CS–OKGM–AgNPs hydrogel demonstrated antibacterial activity and quickest healing process among the animal models, with the regenerated skin closely resembling normal skin resulted from ref. 110.

3.1.4. Gelatin-based BNCs. Gelatin is derived through the irreversible partial hydrolysis of collagen, presenting itself as a biodegradable and biocompatible biopolymer with low antigenicity. It is favored for its rich content of RGD motifs (arginine, glycine, aspartic acid) that could interact with integrins on the cell membrane, enhance cellular proliferation, and facilitate cell adhesion.[104] The clinical applicability of gelatin is limited due to its unfavorable mechanical integrity, inadequate *in vivo* performance, and unregulated active substance release.[111] To address these limitations for full-thickness wound healing, Singh *et al.* engineered a dual cross-linked drug-loaded gelatin/gellan gum-based multifunctional nanocomposite hydrogel. The dually-crosslinked gelatin/gellan gum-based construct was utilized for the co-encapsulation of nanoceria and flurbiprofen (GG/Ge/NC-FLU). On day 14, wounds treated with the developed hydrogel in rats exhibited notably increased collagen deposition and a substantial diminish in the expression of TNF-α and IL-1. In addition, there was an enhanced production of IL-10 and TNF-β3, indicating anti-inflammatory activity. The hydrogel treatment efficiently decreased the expression of the VEGF gene, showing successful promotion of angiogenesis compared to all other groups. This approach was employed to improve localized bioavailability and achieve controlled delivery, with the ultimate goal of effectively addressing infectious chronic wounds.[111]

Nanofibrous nanocomposite structure was developed by incorporating graphene nanosheets into electrospun gelatin/chitosan matrices.[112] The introduction of graphene nanosheets significantly enhanced the porosity of the construct, reaching levels of up to 90% of their volume. This heightened porosity is deemed advantageous for the fabrication of wound dressings, facilitating optimal oxygen and nutrient perfusion within the designated wound-healing region. Furthermore, the incorporation of graphene nanosheets was observed to enhance the antibacterial efficacy of the fabricated nanofiber composite. In this system, gelatin was chosen for its high biocompatibility, biodegradability and hydrophilicity, and low irritability, immunogenicity, and antigenicity behaviors. Combining chitosan and gelatin resulted in the formation of a promising blend composite biomaterial. The inclusion of hydrophilic gelatin enhanced the overall hydrophilicity of chitosan and promoted cell spreading and adhesion on the fabricated biomaterial surface. The synergistic impact of these all components positions the fabricated material as a potent antibacterial wound bandage, capable of safeguarding the wound against potential complications or contamination during the healing process.[112]

Nazarnezhad *et al.* (2022) fabricated a set of nanofibrous constructs that mimic the ECM, comprising gelatin and polycaprolactone (PCL)-based nanofibers.[113] These nanofibers were enriched with platelet lysate, showcasing potential applications in the regeneration of the epidermis. The developed system exhibited extended degradation over a period of 28 days without inducing any cell-toxicity. The poor cell adhesion and proliferation associated with the lack of cell-recognition sites and the hydrophobic nature of PCL was overcome by blending PCL with gelatin. The incorporation of biological molecules, specifically blood derivatives rich in growth factors, not only enhanced cell survival but also demonstrated a protective

response against bacteria. Notably, this result could be attributed to electrostatic interactions between amine groups of platelet lysate and chitosan with the surface negative charge of bacteria. This characteristic positions the construct as a viable option for preventing infections during healing process.[113]

Aboomeirah *et al.* (2022) engineered one-dose bio-replicating skin substitute by preparing wet electrospun nanofibers reinforced with a gelatin/alginate-based nanocomposite.[114] The nanocomposite was crosslinked using *N*-(3-(dimethylamino)-propyl)-*N*′-ethylcarbodiimide hydrochloride (EDC) and strengthened by incorporating fragmented *trans*-ferulic acid (FA)-implemented cellulose acetate/polycaprolactone nanofibers. The fabricated ECM-replicating skin alternatives exhibited effective free-radical scavenging, notable antibacterial potential, porosity, water absorption capability, cytocompatibility, and favorable biodegradability. *In vivo* application of these ECM-replicating skin alternatives demonstrated remarkable wound-healing efficacy, decreasing the wound diameter to 0.95 mm following 15 days of treatment, highlighting their appropriateness for one-time therapy of deep wounds. Furthermore, histological examination of the wound area revealed that the applied skin alternatives not only accelerated the wound healing process but also contributed to enhancing the characteristics of the regenerated skin in the treated region. This was achieved by facilitating the regeneration and deposition of collagen fibers, indicating a positive impact on the structural integrity and overall quality of the healed skin.[114]

3.1.5. Chitosan- and chitin-based BNCs. Chitin is a natural polymer mainly found in marine crustaceans, shrimp, and crabs. It is a linear polysaccharide of D-glucosamine and *N*-acetylglucosamine units linked by β(1–4) glycosidic bonds[115] which is obtained by deacetylation of chitin.[116] Both chitin and chitosan are used very commonly in skin tissue engineering and regenerative medicine due to their desired properties including biocompatibility, biodegradability, affinity to biomolecules, haemostatic activity, ease of processing, and antimicrobial activity.[117–119] They are non-toxic materials with hydrating and analgesic activities. The analgesic activity of chitosan is probably due to proton ions absorption that are released in the inflammatory site, whereas it is due to bradykinin absorption for chitin.[120]

Studies with application of chitin demonstrate that chitin-based dressings support wound healing in various formulations such like mats, membranes, hydrogel formulations as filling agents or wound dressings in cases like surgical tissue defects, trauma cases and in herniorrhaphy.[121,122] Chitin/silk fibroin/TiO_2 bio-nanocomposite was prepared as a biocompatible wound dressing bandage. They prepared an interconnected microporous membrane with antibacterial activity (against *Escherichia coli* (*E. coli*), *Staphylococcus aureus* (*S. aureus*), and *Candida albicans* (*C. albicans*)), blood clotting properties, as well as good mechanical properties. *In vitro* evaluation of the dressings were carried using normal human dermal fibroblast cells, and it was found that the dressings are cytocompatible, and support cell viability, proliferation and attachment. The controlled release of TiO_2 NPs from the hydrogel that was accelerated by the swelling behavior of the hydrogel provided the antibacterial activity for the hydrogel.[123] Chitosan is a more extensively studied polysaccharide used in skin tissue engineering and regenerative medicine, compared to chitin, due to its superior properties such as supporting cell growth, absorbing exudate, minimizing scar formation, and promoting platelet adhesion and aggregation. It is an inexpensive material that could be easily produced, while having properties like hemostatic ability (helps control bleeding) and antibacterial activity (eliminates bacterial infections).[124–127] Degradation products of chitosan are also useful in wound management. Chitooligosaccharides obtained *via* enzymatic or chemical degradation of chitosan, could promote fibroblast proliferation through regulation of mitogen-activated protein kinase pathway and hepatocyte growth factor.[128] Due to these advantages, both polymers are frequently used for the fabrication of BNCs that could be used for skin tissue engineering and regenerative medicine.

In a study, Masud *et al.*, designed a BNC-based wound healing material composed of chitosan–zinc oxide (ZnO)/poly(ethylene glycol) (PEG) crosslinked by sodium tripolyphosphate. Afterwards, an antibiotic, gentamicin sulphate, was loaded within the BNC, and then its wound healing capability was evaluated. ZnO NPs were about 50 nm in diameter and incorporated to enhance antimicrobial properties of the dressing. It is demonstrated that the dressing could provide a moist environment to the wound site. *In vitro* evaluation of the dressings was conducted on the BHK-21 (baby hamster kidney fibroblast cells) and vero cells, and according to the results, the dressings were found to have good biocompatibility. The combination of drug and ZnO NPs provide enhanced antibacterial activity against *E. coli* and *S. enterica*. *In vivo* studies were carried using male nude mice to evaluate wound healing efficacy of the BNC. Drug-loaded BNC, drug-free BNC, and gauze were used in the studies, and contraction, re-epithelialization, and morphology of the wound was evaluated. The antibiotic gentamicin sulphate loaded samples were found to achieve complete wound closure without any scars, and a smoother new skin formation and less scabby. It was while, the nanocomposite without drug and the conventional gauze (used as control) showed 80% and 50% wound closer after 10 days. According to overall results, dressings have a good loading efficiency of drug (76%), as well as good biocompatibility, enhanced antibacterial activity, wound healing properties, without any scar formation compared to commercial wound dressing.[129]

Carboxymethyl chitosan/gelatin-based films were developed with mesoporous silica NPs. *Myrtus communis L.* (Myrtle) aqueous extract was loaded within the NPs that have several phenolic groups and has free radical scavenging ability. According to results, mesoporous silica NPs were found to have many functions such as increasing the tensile strength as well as swelling ratio, and oxygen and water vapor permeability. Also, delayed release of the extract from the NPs resulted in reduced fibroblast cell toxicity. According to histological data in mice

models, collagen percentage and fibroblast migration was found to be increased in the wound area after application of the BNC dressing containing 5% mesoporous silica NPs, which suggest dressings accelerate wound healing in mice model, and may find applications in wound treatment.[130]

An asymmetric wound dressing membrane made of chitosan/polyvinylpyrrolidone (PVP)/nanocellulose was fabricated, featuring a hydrophobic side and a hydrophilic side. The hydrophobic side was achieved through a coating layer of 3% stearic acid. The hydrophobic surface of the BNC material had porous structure, while hydrophilic surface was smooth. It was found that hydrophilic surface showed antibacterial activity against bacterial pathogens, and the hydrophobic side had water repellent and antiadhesion properties against *E. coli*. Chitosan was selected due to its desirable properties such as biocompatibility, biodegradability, intrinsic antimicrobial, and hemostatic property. Poor mechanical properties of chitosan were hindered by preparation of BNCs, where blended materials also serve specific functions in the dressings. For instance, it was found that addition of nanocellulose increased the physicochemical properties of the dressing and also enhanced the antibacterial activity along with chitosan. *In vivo* tests demonstrate that the dressing supports re-epithelialization and wound contraction compared with control studies and compared with the samples without nanocellulose so that the chitosan/PVP/nanocellulose 3%-stearic acid (CPNC3%-S) BNC showed about 100% healing rate after 21 days, while the chitosan/PVP–stearic acid (CP–S) and control group had healing rate of about 80% and 75%, respectively.[131]

3.1.6. Alginate-based BNCs. Alginate is a hydrophilic anionic FDA-approved biopolymer that is fabricated *via* 1 → 4 linkage between β-D-mannuronic acid (M) and α-L-guluronic acid (G). The ratio of M and G blocks have important effect in the properties of this polymer, for instance, the high M-blocks content is preferred in the case of chronic wound healing to produce cytokine production *via* human monocytes.[132,133] Alginate has an excellent water absorption capacity. Native alginate is a bioinert polymer, does not have cell-adhesive moieties, and could inhibit cell adhesion and spreading.[134,135] Due to its numerous advantages such as biocompatibility, non-toxicity, non-immunogenic, low-cost, easy crosslinking, and adjustable gel properties, alginate-based materials are commonly used for many applications including wound healing and skin tissue regenerative.[136,137] A wet and moist environment could be created by alginate materials, that could promote re-epithelialization and reduce scar formation especially for wound healing application.[138]

Nanocomposite sponges of sodium alginate/graphene oxide/polyvinyl alcohol were developed for wound healing applications (Fig. 6).[139] The dressings were formulated as sponges, and the obtained sponges had a uniform pore structure as well as flexibility. They found that porous and interconnected network structure was obtained, and the formulation with 1% graphene oxide had more homogeneous pores. The porous structure of the sponges could promote cell growth, ensure breathability, and improve water absorption capacity of the dressing. When a norfloxacin was encapsulated within the formulation for treatment of bacterial infections, sustained release of the drug was achieved that led to a strong inhibitory effect against both *E. coli* and *S. aureus* (Fig. 6(A)). Wound-healing rate of the samples were assessed on *in vivo* mice model, that showed the fabricated formulation with 1% graphene oxide encapsulating norfloxacin had enhanced healing ability (Fig. 6(B)) and prevented the inflammation in wound area without any toxic effects compared to the BNCs without norfloxacin and the gauze treated wounds. In here, alginate was preferred due to its ability to absorb wound exudate, provide moist environment, and its hemostatic activity, and indeed the wound closure was higher in the BNCs due to lower WVTR rate which is crucial for creating a moist environment in healing. *In vivo* results also demonstrated that drug loaded nanocomposites accelerate wound closure (about 90% wound closer compared with 65% in control), and the wounds were smooth without significant scars (Fig. 6(C) and (D)). The wounds treated with the complete composite showed better skin regeneration *via* exhibiting more generation of hair follicles and blood vessels compared to sodium alginate/graphene oxide (GO)/polyvinyl alcohol (SPG) sponge and control group.[139]

Crosslinked alginate/chitosan nanocomposite sponges were developed using green synthesized carbon dots. Alginate was selected because of its highly water-absorbent, non-stick, cost-effective properties. Beside these, the anionic property of this polymer enables preparation of composites effectively with positively charged chitosan through electrostatic interaction. Carbon dots were selected in preparation of the BNCs; carbon dots less than 10 nm found applications in many areas due to their biocompatibility, hydrophilicity, low cytotoxicity, antibacterial properties, good mechanical properties as well as easy manufacturing. In the study, carbon dots were synthesized, and then used in the fabrication of nanocomposite sponges with chitosan and sodium alginate. The fabricated alginate/chitosan wound dressing showed many advantages like enhancing red blood cell and platelet formation and blood clot production. Also, ECM secretion and tissue granulation were supported by alginate/chitosan dressing. This dressing could absorb the exudate of the wound site, and its antibacterial property supports wound healing. Besides, the incorporation of carbon dots enhanced the porosity of nanocomposite sponge as well as its water absorption and transmission rate, hydrophilicity, and mechanical properties. The sponge transformed into a semi-swelling viscous colloid, potentially leading to capillary blockage. Cytocompatibility tests were carried out with L929 cells, and the results indicated no apparent cytotoxic effects from the nanocomposite sponge. Nanocomposite sponges found hemocompatible, and having hemostatic potential in increasing CD concentrations.[140]

3.1.7. Starch-based BNCs. Starch is a biocompatible, biodegradable, non-toxic polymeric carbohydrate that can mainly be found in two forms: amylose and amylopectin. Amylose is a linear constituent of starch formed by chains of α-(1,4)-linked D-glucopyranose, while amylopectin is a branched polymer formed by α-(1,4)-linked D-glucopyranose linear chains that connected by α-(1,6)-branch linkages. Depending on the starch

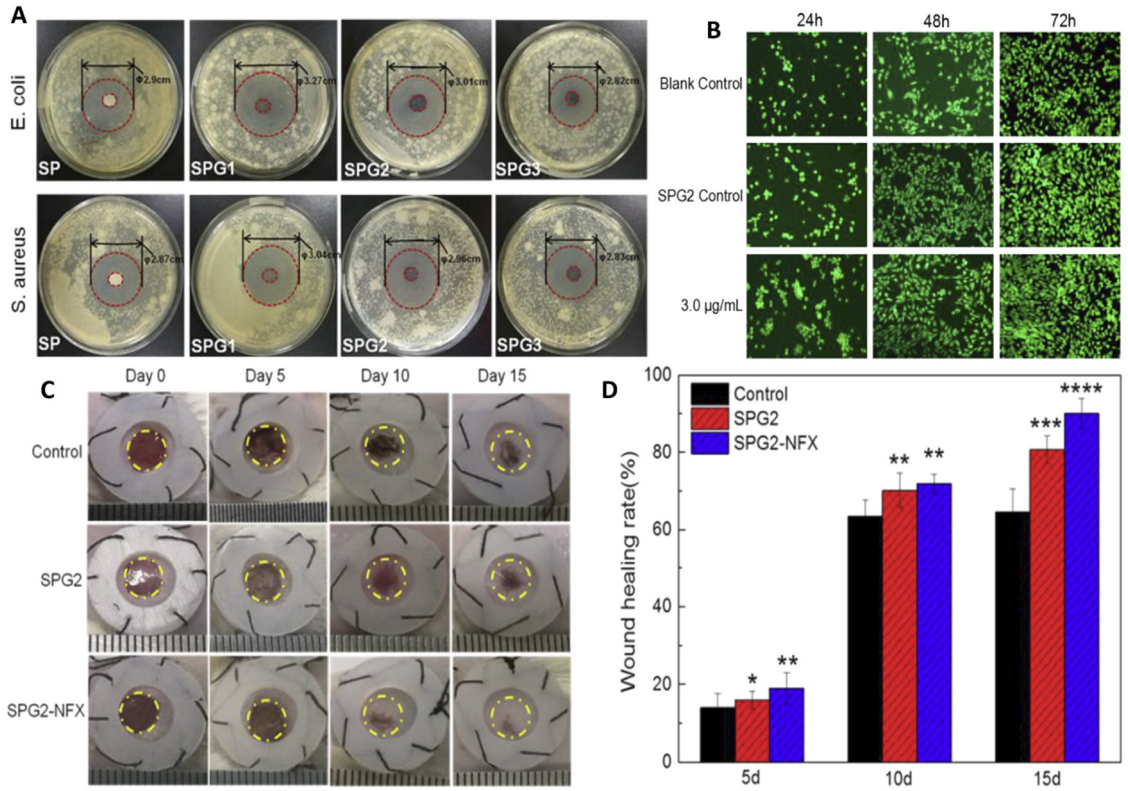

Fig. 6 Preparation and characterization of nanocomposite sponges of sodium alginate/graphene oxide/polyvinyl alcohol (SA/GO/PVA) for wound healing applications. Different amounts of graphene oxide (GO) were used in the studies, and the sponges were referred to as SP, SPG1, SPG2, and SPG3 depending on the GO levels (as 0, 0.5, 1.0 and 2.0 wt% of total solids contents, respectively). (A) *In vitro* antibacterial activity of the samples against *E. coli* and *S. aureus*. (B) NIH 3T3 fibroblast growth cultured using extracts of blank control, SPG2, and SPG2-NFX with different NFX contents for 24, 48, 72 h. (C) Wound-healing image of mice exposed with different treatment. (D) Result of wound healing rate during time and after exposure to different formulation. Reprinted with permission from.[139] Copyright 2019, Elsevier.

source, the ratios of amylose and amylopectin could vary.[141,142] Starch could absorb water, and have gelatinization property which makes them suitable candidates for various applications including applications in tissue engineering, drug delivery, and fabrication of implants.[141] Starch-based scaffolds have been studied for adhesion, proliferation, differentiation, and regeneration of cells.[143] They are usually combined with other polymers and materials to overcome its limitations of this polymer, like low mechanical property, instability, and moisture sensitivity.[144] Cadexomer iodine, oxidized starch, and hydroxyethyl starch are some examples of modified starches used in wound dressing fabrication.[141] Amongst these, cadexomer iodine is roughly used for exudative wounds due to high fluid absorbability, oxidized starch is for electrospinning due to its film-forming ability, and hydroxyethyl starch use as plasma expanders and tissue adhesives.[141] Many types of dressings have been reported with starch including films, hydrogels, sponges, and electrospun scaffolds.[143–146]

A pH-sensitive magnetic starch-based nanocomposite hydrogel was introduced for wound healing applications.[147] The composite hydrogel was synthesized by graft copolymerizing itaconic acid onto starch in the presence of Fe_3O_4 NPs. A model analgesic and anti-inflammatory drug, Guaifenesin, was loaded into the hydrogels, and pH and magnetic field-triggered release of the drug from hydrogels was studied. According to the results, the release of drug from hydrogel network was achieved in a controlled and pH-dependent manner. Guaifenesin release was accelerated by the increase of starch content. When an external magnetic field applied, the percentage of the drug release was significantly enhanced. Cytotoxicity studies showed that HUVEC cell viability was found to be above 88%. *In vivo* studies were carried using healthy male white mice, and wound healing was studied on a full-thickness circular wound model. The study was carried out for 20 days, and it was found that the wound of drug-loaded nanocomposite was healed after 10 days. Also, during the study wound area of nanocomposites were smaller compared to control studies, blank hydrogels, blank nanocomposites, and drug loaded hydrogels. It is assumed that strong adhesion of the starch-based nanocomposite material and the anti-inflammatory property of the drug could be the reason of fast closure of the wounds.[147]

3.1.8. Bacterial cellulose-based BNCs. Bacterial cellulose (BC), a biopolymer synthesized by various bacteria (such as *Acetobacter*, *Rhizobium*, *Gluconacetobacter*, *Agrobacterium*, *Aerobacter*, *Achromobacter*, and *Azotobacter*) is widely used in skin regeneration due to its exceptional properties, including biocompatibility, biodegradability, large surface area, high porosity, high water content, high liquid absorption capacity, high

wet strength, high crystallinity in wet form, and chemical purity. In addition, BC possesses a three-dimensional (3D) network structure similar to the native ECM. However, its endotoxin level must meet the ''generally accepted as safe'' (GRAS) certification established by the FDA.[148–152]

A BC–GO composite film was recently developed using a biological blending self-growth method that naturally incorporated GO during the production of a bacterial cellulose film. This film was then functionalized with dopamine and silver, resulting in the generation of an Ag-pDA (rGO) composite film with good micro-current conductivity and heat generation following applied voltage. The composite film also exhibited excellent antibacterial activity against *E. coli*, with a bactericidal rate of over 84% for more than 72 h, indicating a prolonged antibacterial effect. Moreover, the Ag-pDA/BC (rGO) composite film demonstrated excellent biocompatibility according to *in vitro* cytotoxicity tests. In the live/dead staining test, BC-treated NIH3T3 cells exhibited almost completely green color because of the excellent biocompatibility of BC film alone. Nevertheless, BC(GO) and PDA/BC(GO) slightly inhibited the proliferation NIH3T3 cells (about 2% inhibition). On the surface of wound, presence of AgNPs and so release of Ag^+ ions provided antibacterial and antifungal activity. Presence rGO in the structure of this composite provided photoelectric properties for this film that enable it to treat wound *via* accelerating migration of skin cells in different parts of wound that enhance the healing rate.[153] Similarly, Khan *et al.*, synthesized curcumin-loaded GO-functionalized-BC (GO-f-BC) hydrogel using hydrothermal method. BC and gelatin were chemically crosslinked by tetraethyl orthosilicate (TEOS) as a crosslinker. According to Franz diffusion test, the hydrogels with GO exhibited a slower drug delivery rate than the GO-free hydrogels, while displaying sufficient antibacterial efficacy due to the synergistic effect of the polymer and GO. GO could adhere to bacterial membranes through electrostatic interactions, while the polymeric part of the hydrogels interacted with bacterial phospholipids and lipopolysaccharides to hinder bacterial growth. Both of the hydrogels, with and without GO, exhibited a negligible hemolysis rate (less than 5%) and were found to be hemocompatible. The slight hemolysis observed in GO-included hydrogels was attributed to the twisting effect of GO, which may electrostatically interact with blood cells.[154]

Wan *et al.*,[155] developed BNC hydrogels composed of BC and silver nanowires (AgNWs) through a step-by-step *in situ* biosynthesis process. It showed antibacterial activity against Gram-positive and Gram-negative bacteria *via* affecting cellular membrane of these bacteria. Interestingly, this hydrogel had a better effect on Gram-negative bacteria that was due to the protective effect of lipopolysaccharides, proteins, and lipids that are presented in the structure of Gram-negative. The BC/AgNW dressing with 38.4 wt% AgNWs showed superior expression of cytokeratin-10 and integrin-β4, higher keratinocytes proliferation and epithelial tissues formation, which has been shown to enhance skin regeneration in a mouse model of circular excisional full-thickness wounds.[155] Another study by Gupta *et al.*, utilized a green chemistry approach to produce silver NPs (AgNPs) using an aqueous solution of curcumin and hydroxypropyl-β-cyclodextrin (CUR:HPβCD). These AgNPs were then loaded into biosynthetic BC hydrogels to create hydrogel dressings. The CUR:HPβCD inclusion complex was formed to prevent the hydrophobicity of curcumin, a natural polyphenolic compound with wound-healing properties. The resulting BC hydrogels with CUR:HPβCD demonstrated high cytocompatibility and hemocompatibility, as well as antibacterial activity against three common wound-infecting pathogens: *S. aureus*, *Pseudomonas aeruginosa*, and *Candida auris*.[156]

3.2. Synthetic polymers

3.2.1. Polyvinyl alcohol-based BNCs. Polyvinyl alcohol (PVA) is one of the widely used synthetic polymer in wound dressings due to its biocompatibility, biodegradability, hydrophilicity, mechanical stability, transparency, film-forming characteristics, and ability to maintain a moist environment at the wound site.[149,157] PVA is available in different molecular weights and degrees of hydrolysis as partial (80.0–98.5%), high (>98.5%), and full (100.0%), and can be crosslinked to generate stable hydrogels using methods such as freeze-thawing cycle, electron beam irradiation, or cross-linking agents (*e.g.*, glutaraldehyde).[158,159] PVA possesses several shortcomings, including poor elasticity, rigid structure, limited hydrophilicity, insufficient exudate absorption capacity, and inert bioactivity. Consequently, the development of PVA-based BNCs is a promising approach to improve wound dressing characteristics and enhance bioactivity.[158,160,161]

Crosslinked composite membranes were fabricated by combining PVA, chitosan-loaded $AgNO_3$ NPs, and vitamin E *via* gamma irradiation. After exposing an aqueous solution of PVA to ionizing gamma radiation, free radicals were generated along the polymer chains due to hydrogen abstraction. The –OH and $–NH_2$ groups on the chitosan backbone were potential sites for the reaction, and the formation of radical sites at oxygen and nitrogen atoms was dependent on a high amount of energy to break the O–H and N–H bonds. Hence, radical sites at oxygen and nitrogen atoms were generated by gamma irradiation. The copolymerization of PVA and chitosan radicals resulted in the formation of crosslinked (PVA/Cs) hydrogel membrane. The gelation of these membranes increased significantly with PVA composition, irradiation dose, and glycerol content up to 20%, whereas it decreased with the presence of AgNP due to increased viscosity. The swelling ratio decreased with increasing radiation dose and AgNP amount due to the effects of AgNP and reduced crosslinking degree of the membranes. These BNC membranes exhibited potent antimicrobial activity against *Streptococcus mutans* compared to other bacterial and fungal microorganisms, attributed to the presence of AgNPs *via* affecting the bacterial membrane as well as some of the bacterial enzymes and proteins.[162]

Song and colleagues prepared AgNPs-incorporated PVA/BC hydrogels as wound dressings using a freeze–thaw method. The microstructure of PVA/BC hydrogel exhibited uniform honeycomb pores with diameters of 1–2 μm, while the PVA/BC–Ag composite hydrogels showed more irregularly serrated and

wedge-shaped structure with pore diameters of 3–5 μm, providing better oxygen exchange, moisture retention, and cell adhesion and growth. The mechanical properties of PVA/BC–Ag hydrogels were improved compared to PVA/BC. Moreover, the water absorption capacity of PVA/BC–Ag (approximately 1604.9 ± 58.2%) was higher than PVA/BC hydrogel due to larger pores and higher water-holding capacity of AgNP-incorporated hydrogels. Antibacterial tests demonstrated that PVA/BC–Ag showed remarkable antibacterial activity against both Gram-negative (*E. coli*) and Gram-positive (*S. aureus*) bacteria, with bactericidal rates of 99.72 ± 0.14% and 99.38 ± 0.48%, respectively. All hydrogels exhibited high biocompatibility on L929 mouse skin fibroblasts. Moreover, after 15 days, PVA/BC–Ag groups demonstrated more mature, flat, and thickened epidermis layers with more glands and blood vessels, so that the percentage of reducing wound size in group treated with PVA/BC–Ag3, PVA/BC, and control was about 97.89 ± 0.97, 61.13 ± 5.37%, 47.74 ± 4.13%, respectively.[163]

Zheng *et al.*,[109] designed an electro-conductive hydrogel composed of β-cyclodextrin-embedded Ag NPs (CDAgNPs) containing PVA matrix incorporated free β-cyclodextrin (CD) and β-glucan grafted with hyaluronic acid (HAG) (PVA/CD/HAG/CDAgNP) (Fig. 7(A)). They applied electrical stimulation (ES) to induce tissue reparation. PVA/CD/HAG hydrogel showed low antibacterial efficacy against *E. coli* and *S. aureus* with a killing ratio below 15%, whereas PVA/CD/HAG with CDAgNP killed ≥99.99% of both bacterial strain within 1 and 4 h, respectively (Fig. 7(B)). *In vitro* fibroblast proliferation of PVA/CD/HAG and PVA/CD/HAG/CDAgNP was evaluated with and without ES of 100 mV mm^{-1} over 1 h per day. According to the CCK-8 assay, fibroblasts proliferated well on both materials after 5 days, in the absence of ES ($p > 0.05$). After 3 days, ES accelerated the cell proliferation with both materials, indicating a favorable effect of exogenous electric fields on the physiology and metabolism of fibroblasts. However, higher electroconductivity of PVA/CD/HAG/CDAgNP led to significantly higher cell growth upon ES than PVA/CD/HAG. PVA/CD/HAG/CDAgNP also promoted *in vivo* wound healing and hemostasis in the rat model (Fig. 7(C)). ES improved the healing process, and the PVA15/CD/HAG and PVA15/CD/HAG/CDAgNP groups led to complete skin injury recovery after 10 and 6 days, respectively. This was attributed to the higher electroconductivity of PVA15/CD/HAG/CDAgNP upon ES, which enables better signal transmission, controls cell activities, and accelerates healing. When ES was applied, more developed hair follicle and sebaceous gland systems, the highest volume of collagen fibers, and more efficient epidermal regeneration in the basal, spinous, and granular strata were achieved with the AgNP-containing nanocomposite hydrogel (Fig. 7(D)).[109]

Liu *et al.*,[164] prepared mupirocin (MP) and/or cerium oxide NPs (CeNPs) incorporated PVA/CS nanofiber membrane wound dressing using electrostatic spinning (Fig. 8). The study

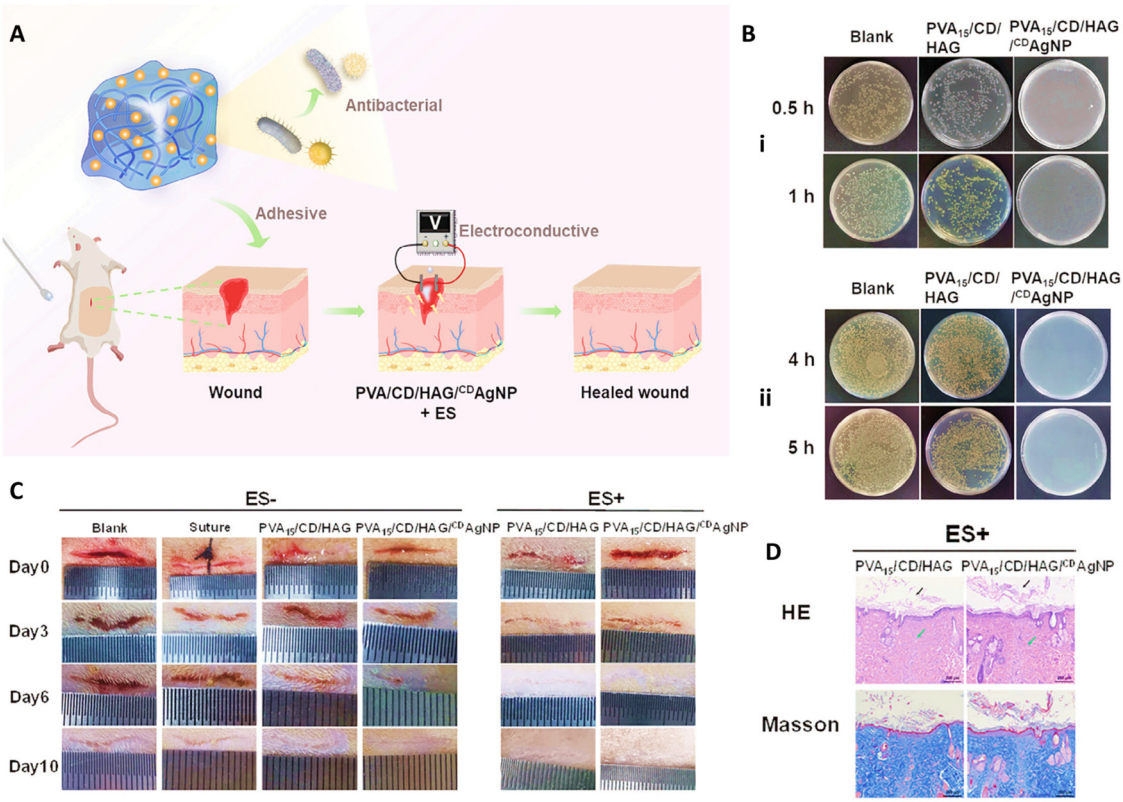

Fig. 7 (A) Schematic image of combination use of PVA/CD/HAG/CDAgNP and electrical stimulation applied for healing wound. (B) Antibacterial activity of PVA15/CD/HAG/CDAgNP against (i) *E. coli* and (ii) *S. aureus*. (C) Wound healing results of different treatment in the presence and absence of ES for 10 days. (D) Histological results of wound after 10 days exposure to different samples. Reprinted with permission from.[109] Copyright 2023, Wiley.

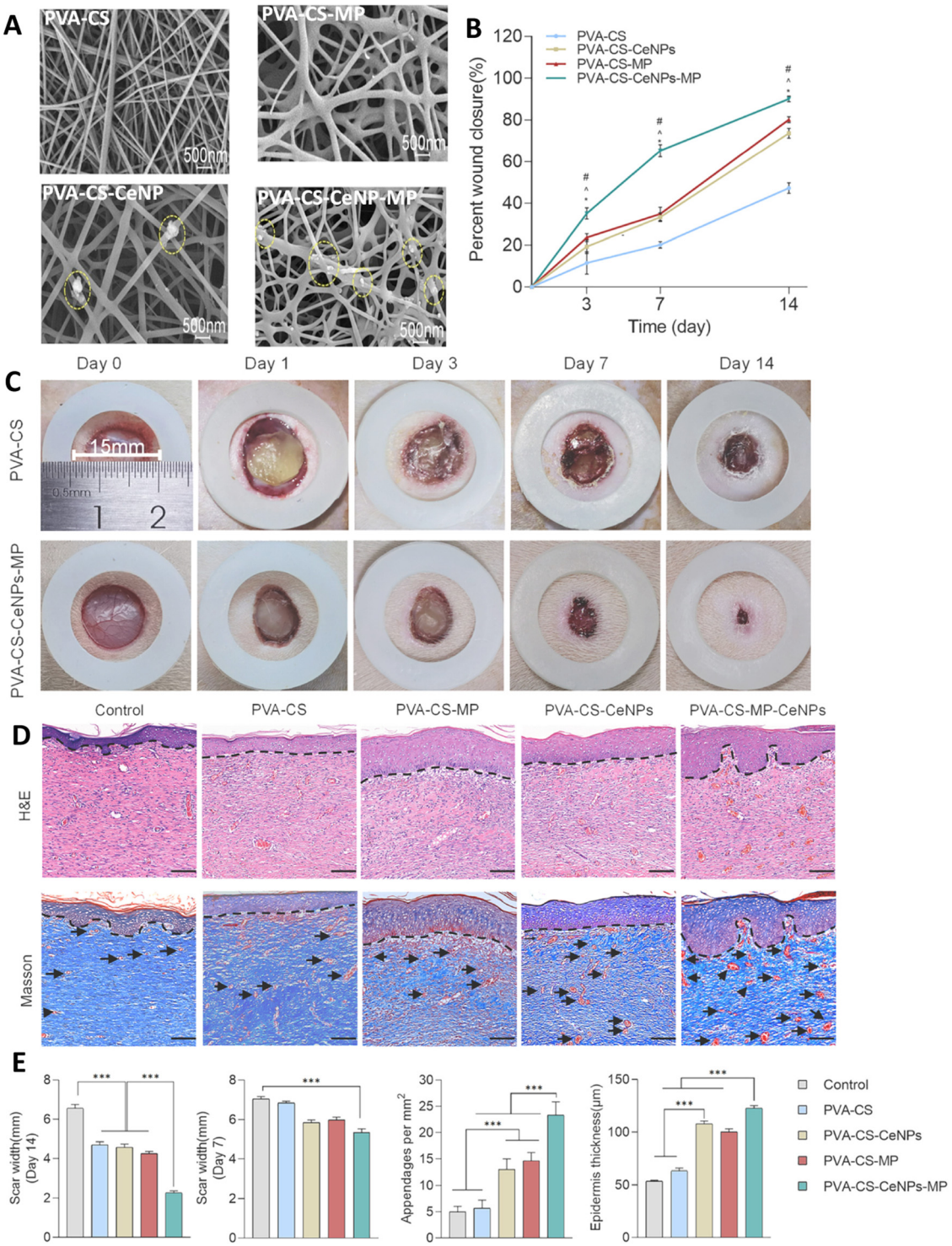

Fig. 8 (A) The SEM image of the PVA–CS, PVA–CS–MP, PVA–CS–CeNPs, and PVA–CS–CeNPs–MP nanofiber dresses; circles show CeNPs. Quantitative analyses (B) and image (C) of wound closure on the wound bed in the CS–PVA, and CS–PVA–CeNPs–MP groups at the predefined time intervals. (D) Representative images of H&E and Masson's trichrome staining. Dashed black lines and black arrows show epidermis and the blood vessels, respectively. (E) The scar widths and blood vessels in the wound areas, and the thicknesses of the epidermal layers of healed wounds treated with the various PVA–CS-based membranes (*$P < 0.05$, ***$P < 0.001$). Reprinted with permission from.[164] Copyright 2023, Elsevier.

reported the controlled release of MP from the PVA/CS nanofiber dressing, resulting in the fast and sustained antibacterial activity against both methicillin-sensitive *Staphylococcus aureus* (MSSA) and methicillin-resistant *Staphylococcus aureus* (MRSA) strains. In addition, the CeNPs displayed a slower release profile, providing favorable reactive oxygen species (ROS) scavenging

efficiency and maintaining a normal physiological level of local ROS. All hydrogels exhibited high cell viability (>90%) after days 3 and 5 on L929 cells, with no significant difference in cell spreading area among the different hydrogels. The efficacy of PVA–CS, PVA–CS–CeNPs, PVA–CS–MP, and PVA–CS–CeNPs–MP electrospun dressings was evaluated in a diabetic wound rat model. PVA–CS–CeNPs–MP showed superior wound closure after 14 days (near 90%), followed by the PVA–CS–MP and PVA–CS–CeNPs groups (about 75% and 70%, respectively). Moreover, PVA–CS–CeNPs–MP demonstrated greater skin regeneration and neovascularization, as seen in Masson's trichrome staining.[164]

Electrospun scaffolds were prepared using PVA, gelatin, and ZnO NPs (0%, 0.5%, and 1%). The addition of 1 wt% ZnO to PVA/gelatin hydrogel slightly increased the water contact angle from 48.874° to 66.282°, but it remained hydrophilic (WCA < 90°). After 14 days of incubation in PBS, the water uptake capacity of PVA/gelatin, PVA/gelatin/ZnO 0.5 wt%, and PVA/gelatin/ZnO 1 wt% were 2057%, 1485%, and 1291%, respectively. Mesenchymal stem cells adhered and spread well on PVA/gelatin/ZnO 1 wt% hydrogel. The survival rate was highest for the control group and PVA/gelatin scaffold possessed greater survival rate than scaffolds containing ZnO NPs. These nanocomposite scaffolds directly inhibited bacterial growth in a dose-dependent manner. PVA/gelatin without ZnO exhibited no inhibition zone, whereas the inhibition zone ranged from 5.5 mm to 1 cm with the presence of 0.5% and 1% ZnO. In here, ZnO NPs could disrupt bacterial membrane *via* electrostatic interactions with the cell wall as well as production of ROSs, and also exhibiting photocatalytic activity that led to producing ROSs and disturbing vital compounds of bacteria.[165]

3.2.2. Poly(lactic acid)-based BNCs. Poly(lactic acid) (PLA) is a prominent FDA approved biopolymer that exhibits favorable biocompatibility, biodegradability, mechanical durability, and elasticity in wound dressing applications.[166,167] The released lactic acid and pH reduction in application site can inhibit bacterial growth, accelerates collagen synthesis, and promotes epithelization.[168–170] However, its hydrophobic nature, that limits its water uptake capacity, weak cellular affinity, and low degradation rate could restrict its usage for wound-related applications.[167,171] To address these issues, researchers have designed PLA-based constructs in combination with various natural polymers and nano structures. For instance, Rapa *et al.*, prepared biocompatible and stable films composed of PLA, collagen, and AgNPs. The roughness of the films was enhanced from 34.4 nm to 57 nm by the presence of 1.5% (w/v) AgNPs. The PLA samples containing Ag NPs showed values of cell viability higher than 100% after 24 h, that slightly decreased after 48 h. Based on cell cycle analysis performed by flow cytometry, the BNC films did not affect cell proliferation as well as exhibited a normal growth rate.[172]

Hybrid nanofibers were designed using PLA and keratin (K)/PVA with the incorporation of natural nanofibrillated chitosan (CHNF)/ZnO NPs (ZnONPs) (CSZ) as the nanofiller. To fabricate nanofibers, PLA solution from one syringe and K/PVA from another one with incorporation of CHNF, CSZ (2 : 1), (1 : 1) and (1 : 2) were electrospun and nanofibers were collected on the rotating collector. The diameter of the K/PVA nanofiber was around 380.48 ± 24 nm, whereas the presence of CHNF/ZnONPs (2 : 1), (1 : 1) and (1 : 2) resulted in the 376.34 ± 29 nm, 369.13 ± 33 nm and 363.68 ± 34 nm in nanofiber diameter, respectively. The recommended scaffold for wound healing was K/PVA : CSZ (2 : 1)–PLA : CSZ (2 : 1) nanofiber with a diameter of 352.50 ± 31 nm, a contact angle of 48 ± 3°, and a tensile strength of 0.96 ± 0.18 MPa. The addition of CHNF to the K/PVA/CS-PLA/CS nanofiber improved cell proliferation significantly than K/PVA-PLA nanofiber ($P \leq 0.05$). The antibacterial activity of K/PVA : CSZ (2 : 1)–PLA : CSZ (2 : 1) against Gram positive and Gram negative bacteria was greater (with inhibition zones of about 33.13 ± 0.67 mm and 25.06 ± 0.24 mm against *S. aureus* and *E. coli* bacteria, respectively) than other scaffolds due to the effect of CHNF and ZnONPs.[173]

3.2.3. Poly (lactic-*co*-glycolic acid)-based BNCs. Poly (lactic-*co*-glycolic acid) (PLGA), a copolymer of poly lactic and poly glycolic acids, is a commonly used biodegradable polymer in biomedical applications due to its commercial availability, degradation in physiological conditions, and potential modifications in physio-chemical and surface properties. Moreover, its use in biomedical applications has been approved by both FDA and European medicines agency (EMA).[174] In addition, PLGA is widely used as a carrier for various small molecules, proteins, and peptides in wound healing applications due to its controlled release ability and adherence to the wound surface. PLGA could promote wound healing by releasing lactate, which stimulates reparative angiogenesis and collagen synthesis.[175,176] For instance, Porporato *et al.* showed that PLGA resulted in a nearly 4.7-fold increase in plasma lactate levels after implantation in mice compared to untreated mice, and also resulted in a 60% decrease in wound area compared to the control group.[177]

Huang *et al.*,[178] incorporated ZnO NPs with PLGA/SF nanofibers for sustained release of NPs on the wound area. Based on SEM images, the nanofibers were generally smooth, and the fiber diameters increased with the increasing ZnO amounts. PLGA/SF nanofibers with ZnO concentration of 0%, 1%, 2%, and 3% showed a stress of 3.21, 4.43, 4.93, and 7.5 MPa, and strain as 102.63, 46.31, 30.56, and 35.7%, respectively. According to CCK8 assay on L929 cells, all membranes were biocompatible, but cell proliferation slightly decreased with increasing ZnO concentration. The nanofibers exhibited mild antioxidant activity which was significantly increased with increasing time. The antioxidant activity is mainly attributed to the amino acids and phenolic side chain of SF. The BNC nanofibers showed antibacterial activity against *E. coli* and *S. aureus* dependent on ZnO concentration. In the rat model, PLGA/SF nanofibers with 3% ZnO facilitated earlier wound closure and provided superior re-epithelialization, granulation tissue formation, collagen deposition, and angiogenesis compared to PLGA/SF nanofibers without ZnO (about 87% wound closer in the case of PLGA/SF nanofibers with 3% ZnO compared with about 71% and 66% closer in the case of PLGA/SF nanofibers and control groups, respectively).[178]

A bifunctional composite scaffold was fabricated consisting of black phosphorus nanosheets (BPNSs) containing collagen

sponge with a PLGA knitted mesh (PLGA–collagen–BPNS) for the treatment of melanoma and skin regeneration. BPNSs demonstrated the ability to initiate photothermal ablation of melanoma cells both *in vitro* and *in vivo* by increasing temperature under near-infrared laser irradiation. The scaffold also accelerated fibroblast proliferation and enhanced the expression of angiogenesis-related genes and genes of ECM components for new skin formation. The porosity and nanostructure of these nanocomposite meshes supported cellular adhesion, migration, proliferation, and cell–cell interactions, while biodegradable components of the BPNSs promoted dermal fibroblast proliferation, angiogenesis, and further skin wound healing.[179]

3.2.4. Polycaprolactone-based BNCs. Polycaprolactone (PCL) is FDA-approved hydrophobic polyester with aliphatic and semi-crystalline structure. It is a biocompatible and biodegradable thermoplastic with high toughness and mechanical strength. However, the slow degradation rate and hydrophobicity of PCL can lead to poor interaction with biological fluids, inadequate cellular adhesion and proliferation, that negatively affect its application and make it important to use it in combination with other materials.[180–182] Rather *et al.*, fabricated cerium oxide NPs (CeNP) functionalized PCL–gelatin nanofiber (PGNPNF) mesh to investigate its antioxidative potential in wound healing. The randomly oriented nanofibers exhibited ~2.6 times decreased in crystallinity compared to pristine PCL, resulting in the rapid degradation of nanofibers and release of CeNP. The BNC meshes showed superoxide dismutase (SOD) mimetic activity and scavenged reactive oxygen species (ROS) by taking advantage of CeNPs. In addition, cell viability and proliferation of 3T3-L1 cells on both PCL–gelatin nanofiber (PGNF) and PGNPNF were increased based on alamar blue assay. However, PGNPNF exhibited ~17% and ~45% higher cell proliferation rate than PGNF after 24 h and 72 h, respectively. This increase in cell proliferation was attributed to decreasing oxidative stress because of the incorporation of CeNP.[183] Similarly, Naseri and coworkers developed electrospun PCL and gelatin fibrous films incorporated CeNP (1.5, 3, and 6% (w/v)) as wound dressing material. The addition of CeNP significantly increased the pore sizes from 12.52 ± 3.54 μm to 47.59 ± 8.25 μm (with 1.5 and 6% (w/v) CeNP, respectively). The PCL/gelatin nanofibrous films with 1.5% CeNP exhibited a water-uptake capacity of 16.87 ± 1.02% and the water vapor transmission rate (WVTR) of 3272 ± 470.51 $g{\cdot}m^{-2}$, while the films with 6% CeNP exhibited a water-uptake capacity of 15.80 ± 0.66% and a WVTR of 3608 ± 170.27 $g{\cdot}m^{-2}$. The film contained 1.5% CeO_2 NPs that had the highest proliferation in L929 cells, and thus, it was used on full-thickness excisional wounds in Wistar rats. After a two-week period, it was determined that nearly 100% wound closure was achieved in the wounds treated with the CeNP-incorporated dressing, while approximately 63% closure was observed in wounds treated with sterile gauze.[184]

Kouser *et al.*,[185] utilized solution casting technique to functionalize the surface of halloysite nanotubes (HNTs) with sodium alginate and reinforce them with PCL, resulting in nanocomposite structures with increased thermal stability, mechanical strength, and crystallinity with an increasing amount of nanofiller. The nanocomposite films showed high cytocompatibility with NIH3T3 mouse fibroblast cells through cell proliferation and adhesion. The PCL film with 5% sodium alginate–HNTs demonstrated the highest cell proliferation, which exhibited a concentration-dependent trend. This was mainly due to the fact that HNTs have a negative charge on their surface and a positive charge in their inner lumen, resulting in significant surface functionalization. HNTs also improved cell adhesion and exhibited superior anti-inflammatory activity compared to pristine PCL films. The scratch assay confirmed the wound closure effect of the nanocomposite films on the rate of cell migration, where 5% nanocomposite films demonstrated the highest migration, indicating enhanced wound closure. The addition of sodium alginate and HNTs in the PCL matrix significantly accelerated cell migration in a concentration-dependent manner. The *in vitro* anti-inflammatory activity of the nanocomposite films was analyzed using human red blood corpuscles membrane stabilization (HRBCMS) method, which showed superior anti-inflammatory activity for nanocomposite compared to pristine PCL films. Based on these results, the nanocomposite films were hemocompatible and suitable for wound healing applications.[185] Some of the other samples are summarized in Table 1.

Natural polymers, such as alginate, hyaluronic acid, chitosan, collagen, gelatin, and silk fibroin, possess unique features that make them effective in enhancing tissue healing due to their similarities to native skin. These polymers offer specific protein-binding sites in their backbone, which facilitates cellular interaction and promotes cellular migration, adhesion, proliferation, and differentiation. In addition, their high biocompatibility, biodegradability, unique texture, and porosity further enhance cellular interactions and re-epithelialization. However, natural polymers also have some drawbacks, such as insufficient mechanical properties, batch-to-batch variations, and the risk of immune responses. In contrast, synthetic polymer-based materials can be designed to meet the structural and mechanical requirements of native ECM. However, the main limitation of using synthetic polymers is the absence of bioactive sites for cellular interactions. To address these issues, a crucial strategy is to use both natural and synthetic polymers with the incorporation of nanosized materials to create multifunctional materials that overcome the shortcomings of both natural and synthetic polymers.

4. Challenges and future prospects

Despite their advantages, BNCs have some limitations that could affect their applications. Controllable blending and stabilization of dispersion are essential to produce BNCs. A primary challenge encountered during the processing of these composites is NPs tendency to aggregation, which is attributed to the unique combination of specific surface area and volume leading to inadequate scattering within the selected formulations.

Table 1 Examples of BNCs used in skin tissue engineering and regenerative medicine in literature

Polymer	Nanostructure	Preparation/method	Cells/microorganisms	Application	Main findings	Ref.
Silk fibroin/poly(ε-caprolactone)	Nanofibrous scaffold	Custom-designed cold plate electrospinning and automatic magnet agitation system.	NIH 3T3 fibroblasts	Artificial dermis	– The rate of healing wounds and the deposition of collagen were found to enhance proportionally with the inclusion of silk fibroin in the formulation. – Desirable spatial cues, surface topography, and surface chemistry for the native cells to infiltrate into the scaffolds. – The wound healing capability of the nanofibrous scaffold is comparable to that of the commercially available Matriderm® artificial dermis.	186
Silk fibroin/ poly(glycerol sebacate)/poly(ε-caprolactone) poly(ε-caprolactone)	Electrospun fiber mat	The nozzle-free electrospinning technique	Human dermal fibroblasts	Artificial skin-like platform	— Favorable *in vitro* fibroblast attachment patterns and optimal growth — A novel promising platform for advancing the development of skin substitute products.	187
Collagen/silk fibroin	TiO_2 NPs	Membranes/freeze drying	– *S. aureus* and *E. coli.* – NIH3T3 fibroblast cells	Skin tissue regeneration	– Antibacterial behavior increased with increasing concentration of TiO_2. – Good biocompatibility and cell proliferation on fibroblasts.	188
Melatonin-loaded collagen/aminated xanthan gum	Bio-capped AgNPs	Bio-hybrid hydrogel scaffold/freeze drying	– *Escherichia coli*, *Bacillus subtilis*, *Staphylococcus aureus*, *Pseudomonas aeruginosa* and multidrug-resistant (MDR) *Klebsiella pneumoniae* – NIH 3T3 fibroblast cells	– Accelerated tissue regeneration in skin defects	– Rapid tissue regeneration, collagen accumulation and angiogenesis at the wound site predominantly due to the synergistic effect of AgNPs and melatonin. – Effective care for various ailments, including infected chronic wounds.	189
Gelatin/hyaluronic acid/polycaprolactone	Hydroxyapatite/ atorvastatin-loaded nanostructured lipid carriers	Membranes	Human dermal fibroblasts	Skin tissue engineering	– Mechanical stability (approximately 90 MPa elastic modulus) more than two-fold of tensile modulus of normal human skin. – Degraded up to 98% after 5 days – Drug release efficiency was in a range of 75–79% for 5 days	190
Chitosan	Halloysite Nanotubes	Pour powder	– Normal human dermal fibroblasts (NHDF) from juvenile foreskin – Murine model	Chronic wound healing	– Better skin reepithelization and reorganization than halloysite nanotubes or chitosan oligosaccharide separately. – Presence of granulation tissue after treatment – Overall skin structure was recovered after 18 days	191
Chitosan, poly(*N*-vinylpyrrolidone)	Titanium dioxide (TiO_2) NPs	Films	– NIH3T3 and L929 fibroblast cells – Albino rat model – Pathogenic bacteria (a loopful of bacterial strains)	Wound healing	– Addition of NPs increases the strength of the composite – Antimicrobial efficacy and good biocompatibility in cell culture studies – Accelerated healing of open excision type wounds in albino rat model compared to gauze, ointment and chitosan treated groups	192
Chitin	Nano ZnO	Micro-porous composite bandages	– Human dermal fibroblast	Wound Healing	– Enhanced swelling, blood clotting and antibacterial activity – Cells attached and penetrated into the interior of the bandages	193
Alginate	Pitavastatin nanovesicles	Hydrogel	– Mongrel dogs	Wound Healing	– High water uptake – Sustained drug release up to 7 days – Promoting wound healing and wound closure – Fast and proper rejuvenation of damaged skin layers compared to plain hydrogel and drug suspension	194

Table 1 (*continued*)

Polymer	Nanostructure	Preparation/method	Cells/microorganisms	Application	Main findings	Ref.
Alginate	Eudragit NPs containing edaravone	Hydrogel	– Diabetic mice model	Chronic wound healing	– Protection and sustained the release of edaravone was achieved. – Promotion of wound healing in a dose-dependent way.	195
Polyvinylidene fluoride and starch mats	Ciprofloxacin loaded on TiO_2 NPs	Electrospun mats	– *Escherichia coli* and *Staphylococcus aureus* – L929 mouse fibroblast cell line	Wound healing	– Fiber diameters thickened by increasing starch – Sustained drug release and antibacterial activity were achieved – Dressings found to be biocompatible	196
Bacterial cellulose	Graphene quantum dots	Hydrogel	– *Staphylococcus aureus*, *Streptococcus agalactiae*, Methicillin-resistant *Staphylococcus aureus*, *Escherichia coli*, and *Pseudomonas aeruginosa*. – Human fibroblasts	Wound healing	– Approximately 11.7 wt% of GQDs loaded in the BC – High water uptake – Dressings exhibited significant inhibition *S. aureus* and *S. agalactiae* and bactericidal effect on Methicillin-resistant *S. aureus*, *E. coli*, and *P. aeruginosa*. – Upregulated expression of endothelial nitric oxide synthase, vascular endothelial growth factor A, matrix metallopeptidase 9, and Vimentin gene in fibroblasts were achieved, enhancing angiogenesis.	197
PVA	Copper oxide, ZnO, and Au NPs	Film	– *E. coli* and *S. aureus* – Mouse embryonic fibroblast (NIH 3T3) cells	Wound healing	– An antibacterial efficacy of 98.7% against *E. coli* and 97.5% against *S. aureus* was achieved under red laser irradiation, with photothermal and photodynamic effect, and released Zn^{2+} and Cu^{2+}. – Fast healing with minimum scarring was shown with film dressings in full-thickness circular rat wound model.	198
PCL	Quercetin loaded graphene oxide NPs	Nanofiber	– *S. aureus* – NIH/3 T3 fibroblast cells	Wound healing	– NIH/3 T3 fibroblast cells showed 95% viability on scaffolds – Cell attachment and proliferation on scaffolds was observed by FESEM	199
PLGA	Silver NPs	Nanofiber – Human dermal fibroblast	– K. pneumonia, *E. coli, and P. aeruginosa and* S. saprophyticus	Wound healing	– Fiber diameters ranged between 487 and 781 nm. – Integration of AgNPs within the fibers was accelerated the mechanical properties comparable to the mechanical properties of the human skin. – Nanofibers demonstrated minimal cytotoxicity. – Antimicrobial activity was shown using three different strains of Gram-positive and Gram-negative bacteria.	200
PLA, PCL	ZnO NPs	Bilayer nanofiber *Capparis spinosa* L. extract loaded PLA/ZnO loaded PCL	– *Staphylococcus aureus* and *Escherichia coli* – L929 cells (mouse fibroblast cell line)	Wound healing	– Bilayer nanofiber membranes showed satisfactory wettability with water contact angle of 130° for outside layer, 72.4° for inner layer. – Nanofibers was not break until reaching 10.69 MPa, much higher than the tensile strengths of the individual layers. – Bilayer nanofiber membranes significantly prevented bacterial growth. – They highly promoted cell growth.	201

Moreover, increasing the amount of nanofiller leads to a reduction in the toughness and strength of the BNC, resulting in production of a more brittle material. In addition, the viscosities of BNCs also elevate with increasing the nanofiller content, posing difficulties in the manufacturing process. Therefore, it is critical to optimize the properties of NPs and its amounts first, and then use it for the preparation of hydrogels. For instance, NPs could be covered with some polymers to prevent their aggregation, first, and then be applied in the structure of the BNC. Or some techniques like agitation or sonication could be applied for enhancing their dispersion during preparation step. The important points that should be considered here is that these modification and techniques should not have any effect on the properties of the NPs or nanocomposite.

The other challenge is related to the long-term safety of nanomaterials used in the structure of BNCs. Indeed, several types of nanomaterials are widely used for fabrication of different types of BNCs in recent research that could impact cell viability and tissue interactions. Achieving a delicate balance between promoting wound healing and avoiding adverse effects requires extensive research to understand the intricate dynamics of these materials within the biological environment. Overcoming these biocompatibility challenges is imperative to ensure the safety and efficacy of BNCs in wound healing applications and so substantial efforts are needed to generate new knowledge about their impact on human health before establishing regulatory frameworks in this field.[202]

In the case of natural polymers, the variability in their source, probability of contamination, lack of proper mechanical stability, uncontrollable degradation rate, and difficulty in processing are challenges that could affect the performance of BNCs.[203] To overcome these limitations, it is critical to introduce and use standard methods for the extraction and purification of natural polymers to ensure their quality and reduce any possibility of contamination. Moreover, cross linking or combination use these polymers with other compounds could enhance their mechanical and degradation properties. On the other hand, synthetic polymers have challenges in their cost, environmental impact, and toxicity, that could be related to their byproduct. These also make it important to develop new cost-effective methods for producing these polymers and use of non-toxic monomers to eliminate the probability of producing toxic byproducts. Besides, these polymers could be combined and modified with other materials to reducing their effect on environment as well as modifying their degradation ability.

In the case of a complete BNCs, one of the main challenges is related to tuning their mechanical properties of BNCs due to their effectiveness in wound healing process. Indeed, skin, like other tissues in the body, have its specific mechanical properties such as elasticity, tensile strength, and stiffness and the BNCs used in wound healing need to match these properties to ensure proper integration and functionality. It should maintain the structural integrity of wound dressings during application and throughout the healing process. If the material is too weak, it may break down prematurely and compromising the healing environment. It also could ensure that the dressing is not too stiff or too loose, enhancing patient comfort. Moreover, tuning the mechanical properties could affects the degradation profile, ensuring the material provides support as long as needed and then safely degrades without causing harm. Mechanical property of BNCs also can influence cell behavior, including attachment, proliferation, and differentiation. Optimal mechanical properties can create a conducive environment for cells to grow and heal the wound effectively.

Scalability and cost-effectiveness pose challenges for the widespread adoption of BNCs in wound care. The production of these materials often involves sophisticated processes and specialized equipment, leading to higher production costs. This limits their accessibility, especially in resource-constrained environments, where cost-effective solutions are essential. Addressing scalability issues and finding economically viable production methods are crucial steps in enhancing the practical utility of BNCs for wound healing on a larger scale. However, due to the possibility of using diverse materials for the fabrication of BNCs, they could be a good candidate for the fabrication of scaffolds that have the capability of mimicking the ECM of skin resembling the natural microenvironment, fostering cell adhesion, proliferation, and differentiation. In addition, the incorporation of bioactive NPs can further enhance the regenerative potential by promoting angiogenesis and modulating immune responses. This personalized approach holds the promise of accelerating wound healing and minimizing scarring, ultimately leading to more effective and aesthetically pleasing outcomes for patients undergoing skin regeneration procedures. They could be fabricated using intelligent materials with the ability of responding to the specific physiological triggers, enabling dynamic interactions with the surrounding tissue. Smart BNCs may incorporate sensors for real-time monitoring of the healing process, allowing for timely adjustments to the therapeutic strategy. Moreover, the controlled release of growth factors or drugs from these materials can be precisely regulated, optimizing the healing trajectory, and minimizing potential side effects. On the other hand, there is a growing emphasis on sustainability in materials selection. Researchers are increasingly exploring the integration of eco-friendly and renewable resources in the fabrication of these advanced bionanomaterials. The shift towards sustainable materials not only aligns with global environmental goals but also addresses concerns related to the biocompatibility and long-term effects of synthetic polymers. Utilizing biodegradable and naturally sourced components for BNCs not only reduces the environmental impact but also ensures that the materials are compatible with the body's natural processes. By incorporating sustainable elements, the future of skin regeneration technologies aims not only to promote tissue healing but also to contribute to a more environmentally conscious and ethical approach in the development of next-generation biomedical solutions.[204–206]

As research in BNCs progresses, the convergence of nanotechnology and regenerative medicine holds immense potential for transforming the landscape of skin repair and regeneration. Designing BNCs that closely mimic the natural extracellular

matrix is crucial for effective tissue regeneration. The composition, structure, and bioactive cues of the BNCs must be carefully tailored to promote cell adhesion, migration, and differentiation. Controlling the degradation rate of BNCs is critical to match the healing timeline of the injured tissue. An excessively slow degradation rate may hinder tissue regeneration, while rapid degradation can compromise the scaffold's ability to provide mechanical support. Notably, clinical translation studies provide valuable insights into the real-world performance of BNCs, helping to validate their effectiveness and safety. Conducting rigorous preclinical and clinical studies, addressing ethical considerations, and ensuring affordability are crucial for successful clinical translation. These studies also contribute to optimizing product formulation, dosing, and delivery methods.

Another crucial challenge that needs to be addressed is regulatory approval procedures. Understanding the regulatory landscape for BNCs in wound healing applications involves a precise, multifaceted approval process to ensure safety and efficacy. This process is overseen by key regulatory bodies, such as the FDA (dood and drug administration) and EMA (European medicines agency). The journey begins with extensive preclinical testing, including cytotoxicity, hemocompatibility, and animal studies, to assess biocompatibility, toxicity, and therapeutic potential. Successful preclinical outcomes pave the way for multi-phase clinical trials to evaluate safety, dosage, efficacy, and side effects in progressively larger patient cohorts. Adhering to good manufacturing practices (GMP) and precise quality control is critical, involving comprehensive documentation and consistent batch testing. The conclusion of this data in a detailed regulatory report, encompassing technical files, clinical results, and risk management analyses, is submitted for approval. Post-market surveillance ensures long-term safety and efficacy through adverse event reporting and periodic safety updates. By precisely addressing these regulatory challenges, developers can advance BNCs from lab to clinic, offering innovative, safe, and effective solutions for wound healing and skin regeneration.

5. Conclusion

In this review, we have discussed the application of different types of BNCs for wound healing and skin regeneration. In this context, first different phases of wound healing were discussed; then, BNCs based on the type of their biopolymer were introduced. They mostly composed of a biopolymeric hydrogel used alone or in combination with other polymers that were applied to improve the physicochemical properties of the hydrogel, and a nanomaterial with intrinsic antimicrobial or antioxidant ability that prevented the infections in the site of wound and accelerated healing process *via* managing inflammatory phase. These composites also accelerated the healing process of wound in comparison to their control groups *via* enhancing re-epithelialization, promoting tissue granulation and collagen deposition, and inducing neovascularization that finally led to the tissue regeneration. However, like other materials, these substances face several challenges. Among the most significant concerns are those related to the application of nanomaterials and scalability issues, that make it crucial to conduct more research to fully understand these materials and their applications. Overall, BNCs offer exciting prospects in advanced wound healing and smart wound dressings. These materials, formed by combining biopolymers and NPs, possess unique properties that can develop wound healing and smart wound dressings. They can be used in the development of smart dressings with sensors and drug delivery systems, enabling real-time monitoring and targeted treatment.

Conflicts of interest

Authors declare no conflict of interest.

References

1 J. Bramhill, S. Ross and G. Ross, *Int. J. Environ. Res. Public Health*, 2017, **14**, 66.
2 L. Suamte, A. Tirkey and P. J. Babu, *Smart Mater. Med.*, 2023, **4**, 243–256.
3 A. Das, T. Ringu, S. Ghosh and N. Pramanik, *Polym. Bull.*, 2023, **80**, 7247–7312.
4 M. Jain and K. Matsumura, *J. Biomed. Mater. Res., Part A*, 2016, **104**, 1379–1386.
5 L. Moretti, J. Stalfort, T. H. Barker and D. Abebayehu, *J. Biol. Chem.*, 2022, **298**, 101530.
6 H. H. C. de Lima, V. L. Kupfer, M. P. Moisés, M. R. Guilherme, J. D. Rinaldi, S. L. Felisbino, A. F. Rubira and A. W. Rinaldi, *Carbohydr. Polym.*, 2018, **196**, 126–134.
7 M. Rahim, M. R. H. Mas Haris and N. U. Saqib, *Biophys. Rev.*, 2020, **12**, 1223–1231.
8 N. Kučuk, M. Primožič, Ž. Knez and M. Leitgeb, *Int. J. Mol. Sci.*, 2023, **24**, 3188.
9 M. Alavi and A. Nokhodchi, *Carbohydr. Polym.*, 2020, **227**, 115349.
10 Z. Zhang, J. Ma, T. Xu, T. Wang, X. Jia, J. Lin, C. Lv, L. Cao, Y. Ying, L. Ji, S. Wang and C. Fu, *Adv. Healthcare Mater.*, 2024, 2401005.
11 B. Xu, A. Li, R. Wang, J. Zhang, Y. Ding, D. Pan and Z. Shen, *Adv. Funct. Mater.*, 2021, **31**, 2105265.
12 J. Liu, M. Cao, L. Li, X. Xu, J. Zheng, W. Yao and X. Hou, *Giant*, 2022, **10**, 100100.
13 Z. Zhang, J. Ma, T. Xu, T. Wang, X. Jia, J. Lin, C. Lv, L. Cao, Y. Ying, L. Ji, S. Wang and C. Fu, *Adv. Healthcare Mater.*, 2024, 2401005.
14 A. M. Diez-Pascual, *Polymers*, 2021, **9**, 260.
15 M. Râpă, L. M. Stefan, T. Zaharescu, A.-M. Seciu, A. A. Turcanu, E. Matei, A. M. Predescu, I. Antoniac and C. Predescu, *Appl. Sci.*, 2020, **10**, 2265.
16 S. Sharma, A. Malik and P. Gupta, in *Bionanocomposites in Tissue Engineering and Regenerative Medicine*, ed. S. Ahmed and Annu, Woodhead Publishing, 2021, pp. 507–532, DOI: **10.1016/B978-0-12-821280-6.00021-0**.

17 M. R. Alam, S. Alimuzzaman, M. A. Shahid, F.-E. Karim and M. E. Hoque, *J. Biomater. Sci., Polym. Ed.*, 2023, **34**, 1517–1538.
18 C. Oliveira, D. Sousa, J. A. Teixeira, P. Ferreira-Santos and C. M. Botelho, *Front. Bioeng. Biotechnol.*, 2023, **11**, 1136077.
19 C. Belda Marín, V. Fitzpatrick, D. L. Kaplan, J. Landoulsi, E. Guénin and C. Egles, *Front. Chem.*, 2020, **8**, 604398.
20 M. A. Shalaby, M. M. Anwar and H. Saeed, *J. Polym. Res.*, 2022, **29**, 91.
21 P. Du, X. Chen, Y. Chen, J. Li, Y. Lu, X. Li, K. Hu, J. Chen and G. Lv, *Heliyon*, 2023, **9**, e13506.
22 J. Liu, X. Xie, T. Wang, H. Chen, Y. Fu, X. Cheng, J. Wu, G. Li, C. Liu and H. Liimatainen, *ACS Appl. Mater. Interfaces*, 2023, **15**, 12696–12707.
23 P. Feng, Y. Luo, C. Ke, H. Qiu, W. Wang, Y. Zhu, R. Hou, L. Xu and S. Wu, *Front. Bioeng. Biotechnol.*, 2021, **9**, 650598.
24 H. L. Loo, B. H. Goh, L.-H. Lee and L. H. Chuah, *Asian J. Pharm. Sci.*, 2022, **17**, 299–332.
25 F. Leone, M. Firlak, K. Challen, W. Bonnefin, B. Onida, K. L. Wright and J. G. Hardy, *J. Funct. Biomater.*, 2019, **10**, 50.
26 H. Moustafa, H. E. Nasr and A. M. Youssef, *Biomass Convers. Biorefin.*, 2022, 1–13, DOI: **10.1007/s13399-022-03403-2**.
27 M.-B. Coltelli, L. Aliotta, A. Vannozzi, P. Morganti, L. Panariello, S. Danti, S. Neri, C. Fernandez-Avila, A. Fusco, G. Donnarumma and A. Lazzeri, *J. Funct. Biomater.*, 2020, **11**, 21.
28 M. Rodrigues, N. Kosaric, C. A. Bonham and G. C. Gurtner, *Physiol. Rev.*, 2019, **99**, 665–706.
29 N. X. Landén, D. Li and M. Ståhle, *Cell. Mol. Life Sci.*, 2016, **73**, 3861–3885.
30 H. E. desJardins-Park, S. Mascharak, M. S. Chinta, D. C. Wan and M. T. Longaker, *Front. Physiol.*, 2019, **10**, 322.
31 A. Kowalczyk, P. Kleniewska, M. Kolodziejczyk, B. Skibska and A. Goraca, *Arch. Immunol. Ther. Exp.*, 2015, **63**, 41–52.
32 A. Scridon, *Int. J. Mol. Sci.*, 2022, **23**, 12772.
33 B. P. Nuyttens, T. Thijs, H. Deckmyn and K. Broos, *Thromb. Res.*, 2011, **127**, S26–S29.
34 M. E. Quach, W. Chen, Y. Wang, H. Deckmyn, F. Lanza, B. Nieswandt and R. Li, *J. Thromb. Haemostasis*, 2021, **19**, 2044–2055.
35 G. S. Schultz, G. A. Chin, L. Moldawer and R. F. Diegelmann, *Mechanisms of vascular disease: a reference book for vascular specialists*, 2011, p.423.
36 P. Martin, *Science*, 1997, **276**, 75–81.
37 H. N. Wilkinson and M. J. Hardman, *Open Biol.*, 2020, **10**, 200223.
38 T. Velnar, T. Bailey and V. Smrkolj, *J. Int. Med. Res.*, 2009, **37**, 1528–1542.
39 J. S. Roh and D. H. Sohn, *Immune Netw.*, 2018, **18**, e27.
40 K. Ashina, Y. Tsubosaka, T. Nakamura, K. Omori, K. Kobayashi, M. Hori, H. Ozaki and T. Murata, *PLoS One*, 2015, **10**, e0132367.
41 S. Čejková, I. Králová-Lesná and R. Poledne, *Cor et Vasa*, 2016, **58**, e419–e425.
42 T. Yukami, M. Hasegawa, Y. Matsushita, T. Fujita, T. Matsushita, M. Horikawa, K. Komura, K. Yanaba, Y. Hamaguchi and T. Nagaoka, *J. Leukoc. Biol.*, 2007, **82**, 519–531.
43 M. Subramaniam, S. Saffaripour, L. Van De Water, P. S. Frenette, T. N. Mayadas, R. O. Hynes and D. D. Wagner, *Am. J. Pathol.*, 1997, **150**, 1701.
44 M. Metzemaekers, M. Gouwy and P. Proost, *Cell. Mol. Immunol.*, 2020, **17**, 433–450.
45 S. A. Eming, P. Martin and M. Tomic-Canic, *Sci. Transl. Med.*, 2014, **6**, 265sr266.
46 T. Liu, L. Zhang, D. Joo and S.-C. Sun, *Signal Transduction Targeted Ther.*, 2017, **2**, 1–9.
47 J. G. Filep and A. Ariel, *Am. J. Physiol.: Cell Physiol.*, 2020, **319**, C510–C532.
48 M. T. Masucci, M. Minopoli, S. Del Vecchio and M. V. Carriero, *Front. Immunol.*, 2020, **11**, 1749.
49 F. H. Pilsczek, D. Salina, K. K. Poon, C. Fahey, B. G. Yipp, C. D. Sibley, S. M. Robbins, F. H. Green, M. G. Surette and M. Sugai, *J. Immunol.*, 2010, **185**, 7413–7425.
50 Y. Ge, M. Huang and Y.-M. Yao, *Front. Cell Dev. Biol.*, 2022, **10**, 839248.
51 A. Hassanshahi, M. Moradzad, S. Ghalamkari, M. Fadaei, A. J. Cowin and M. Hassanshahi, *Cells*, 2022, **11**, 2953.
52 B. A. Shook, R. R. Wasko, G. C. Rivera-Gonzalez, E. Salazar-Gatzimas, F. López-Giráldez, B. C. Dash, A. R. Muñoz-Rojas, K. D. Aultman, R. K. Zwick and V. Lei, *Science*, 2018, **362**, eaar2971.
53 P. Olczyk, Ł. Mencner and K. Komosinska-Vassev, *BioMed Res. Int.*, 2014, **2014**, 1–8.
54 R. Goldman, *Adv. Skin Wound Care*, 2004, **17**, 24–35.
55 I. A. Darby, B. Laverdet, F. Bonté and A. Desmoulière, *Clin., Cosmet. Invest. Dermatol.*, 2014, 301–311.
56 F. Cialdai, C. Risaliti and M. Monici, *Front. Bioeng. Biotechnol.*, 2022, **10**, 958381.
57 X. Li, Y. Yang, B. Zhang, X. Lin, X. Fu, Y. An, Y. Zou, J.-X. Wang, Z. Wang and T. Yu, *Signal Transduction Targeted Ther.*, 2022, **7**, 305.
58 P. Bao, A. Kodra, M. Tomic-Canic, M. S. Golinko, H. P. Ehrlich and H. Brem, *J. Surg. Res.*, 2009, **153**, 347–358.
59 G.-H. Fong, *J. Mol. Med.*, 2009, **87**, 549–560.
60 S. Ramakrishnan, V. Anand and S. Roy, *J. Neuroimmune Pharmacol.*, 2014, **9**, 142–160.
61 A. Weidemann and R. Johnson, *Cell Death Differ.*, 2008, **15**, 621–627.
62 M. L. Usui, J. N. Mansbridge, W. G. Carter, M. Fujita and J. E. Olerud, *J. Histochem. Cytochem.*, 2008, **56**, 687–696.
63 I. Pastar, O. Stojadinovic, N. C. Yin, H. Ramirez, A. G. Nusbaum, A. Sawaya, S. B. Patel, L. Khalid, R. R. Isseroff and M. Tomic-Canic, *Adv. Wound Care*, 2014, **3**, 445–464.
64 N. Akombaetwa, A. Bwanga, P. A. Makoni and B. A. Witika, *Polymers*, 2022, **14**, 2931.
65 A. C. d O. Gonzalez, T. F. Costa, Z. d A. Andrade and A. R. A. P. Medrado, *An. Bras. Dermatol.*, 2016, **91**, 614–620.
66 F. V. Borbolla-Jiménez, S. I. Peña-Corona, S. J. Farah, M. T. Jiménez-Valdés, E. Pineda-Pérez, A. Romero-

Montero, M. L. Del Prado-Audelo, S. A. Bernal-Chávez, J. J. Magaña and G. Leyva-Gómez, *Pharmaceutics*, 2023, **15**, 1914.
67 D. Singh, V. Rai and D. K. Agrawal, *Cardiol. Cardiovasc. Med.*, 2023, **7**, 5.
68 R. B. Diller and A. J. Tabor, *Biomimetics*, 2022, **7**, 87.
69 A. E. Rivera and J. M. Spencer, *Clin. Dermatol.*, 2007, **25**, 39–48.
70 H. A. Wallace, B. M. Basehore and P. M. Zito, *Wound Healing Phases*, StatPearls Publishing, Treasure Island (FL), 2019.
71 P. Aramwit, *Introduction to biomaterials for wound healing*, Elsevier Ltd, 2016.
72 G. Yaşayan, E. Alarçin, A. Bal-Öztürk and M. Avci-Adali, in *Studies in Natural Products Chemistry*, ed. R. Atta ur, Elsevier, 2022, **74**, pp. 367–441.
73 B. Mordorski and T. Prow, *Curr. Dermatol. Rep.*, 2016, **5**, 278–286.
74 B. Arora, R. Bhatia and P. Attri, in *New Polymer Nanocomposites for Environmental Remediation*, ed. C. M. Hussain and A. K. Mishra, Elsevier, 2018, pp. 699–712, DOI: 10.1016/B978-0-12-811033-1.00027-5.
75 X. Wang, J. Chang and C. Wu, *Appl. Mater. Today*, 2018, **11**, 308–319.
76 I. Gholamali and M. Yadollahi, *Regener. Eng. Transl. Med.*, 2021, **7**, 129–146.
77 V. G. Bhat, S. P. Masti, S. S. Narasagoudr, R. B. Chougale, P. Kumar and A. B. Vantamuri, *Chem. Data Collect.*, 2023, **44**, 101009.
78 F. N. Harandi, A. C. Khorasani, S. A. Shojaosadati and S. Hashemi-Najafabadi, *Surf. Interfaces*, 2022, **28**, 101592.
79 L. Qi, K. Ou, Y. Hou, P. Yuan, W. Yu, X. Li, B. Wang, J. He, S. Cui and X. Chen, *Mater. Des.*, 2021, **201**, 109461.
80 M. Heydari-Majd, B. Ghanbarzadeh, M. Shahidi-Noghabi, A. Abdolshahi, S. Dahmardeh and M. Malek Mohammadi, *Polym. Bull.*, 2022, **79**, 97–119.
81 Z. Chu, T. Zhao, L. Li, J. Fan and Y. Qin, *Materials*, 2017, **10**, 659.
82 A. Dhasmana, L. Singh, P. Roy and N. C. Mishra, *Mater. Sci. Eng., C*, 2019, **97**, 313–324.
83 P. Dam, S. Altuntas, R. Mondal, J. R. V. Baudrit, A. Kati, S. Ghorai, A. Sadat, D. Gangopadhyay, S. Shaw and O. L. Franco, *Mater. Lett.*, 2022, **327**, 133024.
84 B.-M. Min, G. Lee, S. H. Kim, Y. S. Nam, T. S. Lee and W. H. Park, *Biomaterials*, 2004, **25**, 1289–1297.
85 M. Gholipourmalekabadi, S. Sapru, A. Samadikuchaksaraei, R. L. Reis, D. L. Kaplan and S. C. Kundu, *Adv. Drug Delivery Rev.*, 2020, **153**, 28–53.
86 K. Chen, Y. Li, Y. Li, W. Pan and G. Tan, *Macromol. Biosci.*, 2023, **23**, 2200380.
87 F. A. Sheikh, H. W. Ju, J. M. Lee, B. M. Moon, H. J. Park, O. J. Lee, J.-H. Kim, D.-K. Kim and C. H. Park, *Nanomedicine*, 2015, **11**, 681–691.
88 Q. Wang, S. Zhou, L. Wang, R. You, S. Yan, Q. Zhang and M. Li, *Composites, Part B*, 2021, **224**, 109165.
89 S. Gao, X. Xiong, H. Xie, P. Li, F. Kong, Y. Fan, S. Meng, J. Yuan and Q. Jiang, *Process Biochem.*, 2023, **134**, 218–231.
90 P. Farshi, R. Salarian, M. Rabiee, S. Alizadeh, M. Gholipourmalekabadi, S. Ahmadi and N. Rabiee, *Polym. Eng. Sci.*, 2022, **62**, 2741–2749.
91 X. Yang, S. He, J. Wang, Y. Liu, W. Ma, C.-Y. Yu and H. Wei, *Int. J. Biol. Macromol.*, 2023, **242**, 124872.
92 Y. Fu, J. Zhang, H. Lin and A. Mo, *Mater. Sci. Eng., C*, 2021, **118**, 111367.
93 R. Cassano, F. Curcio, R. Sole and S. Trombino, *Polysaccharide Hydrogels for Drug Delivery and Regenerative Medicine*, Elsevier, 2024, pp.35–46.
94 N. K. Dehkordi, M. Minaiyan, A. Talebi, V. Akbari and A. Taheri, *Biomed. Mater.*, 2019, **14**, 035003.
95 S. Li, Q. Dong, X. Peng, Y. Chen, H. Yang, W. Xu, Y. Zhao, P. Xiao and Y. Zhou, *ACS Nano*, 2022, **16**, 11346–11359.
96 J. Hu, M. Tao, F. Sun, C. Chen, G. Chen and G. Wang, *Int. J. Biol. Macromol.*, 2022, **222**, 55–64.
97 Y. Yang, Z. Dong, M. Li, L. Liu, H. Luo, P. Wang, D. Zhang, X. Yang, K. Zhou and S. Lei, *Int. J. Nanomed.*, 2020, 8231–8247.
98 Y. Zhou, Y. Fan, Z. Chen, Z. Yue and G. Wallace, *Biofabrication*, 2021, **14**, 015004.
99 R. Chang, D. Zhao, C. Zhang, K. Liu, Y. He, F. Guan and M. Yao, *Int. J. Biol. Macromol.*, 2023, **226**, 870–884.
100 R. Kashimoto, Y. Kamei, S. Nonaka, Y. Kondo, S. Yamamoto, S. Furukawa, A. Ohashi and A. Satoh, *Dev. Biol.*, 2023, **498**, 14–25.
101 A. A. Chaudhari, K. Vig, D. R. Baganizi, R. Sahu, S. Dixit, V. Dennis, S. R. Singh and S. R. Pillai, *Int. J. Mol. Sci.*, 2016, **17**, 1974.
102 C. Valentino, B. Vigani, G. Zucca, M. Ruggeri, C. Boselli, A. I. Cornaglia, L. Malavasi, G. Sandri and S. Rossi, *Int. J. Biol. Macromol.*, 2023, **242**, 125000.
103 M. R. Alam, M. A. Shahid, S. Alimuzzaman and A. N. Khan, *Adv. Biomed. Eng.*, 2022, 100064.
104 E. Sharifi, S. Yousefiasl, N. Laderian, N. Rabiee, P. Makvandi, S. Pourmotabed, M. Ashrafizadeh, F. Famil-sattarian and W. Fang, *Int. J. Biol. Macromol.*, 2023, **251**, 125898.
105 C. Kalirajan and T. Palanisamy, *Adv. Healthcare Mater.*, 2020, **9**, 2000247.
106 C. Kalirajan and T. Palanisamy, *J. Mater. Chem. B*, 2019, **7**, 5873–5886.
107 P. Khadivar, S. Khajeniazi and A. Karimi, *J. Mater. Res. Technol.*, 2022, **19**, 3966–3979.
108 N. Ribeiro, A. Sousa, C. Cunha-Reis, A. L. Oliveira, P. L. Granja, F. J. Monteiro and S. R. Sousa, *Nanomedicine*, 2021, **33**, 102353.
109 W. Zheng, W. Yang, W. Wei, Z. Liu, P. L. Tremblay and T. Zhang, *Adv. Healthcare Mater.*, 2023, 2303138.
110 H. Gu, H. Li, L. Wei, J. Lu and Q. Wei, *Regener. Biomater.*, 2023, **10**, rbad018.
111 H. Singh, I. Yadav, W. M. Sheikh, A. Dan, Z. Darban, S. A. Shah, N. C. Mishra, S. Shahabuddin, S. Hassan and S. M. Bashir, *Int. J. Biol. Macromol.*, 2023, **251**, 126349.
112 I. H. Ali, A. Ouf, F. Elshishiny, M. B. Taskin, J. Song, M. Dong, M. Chen, R. Siam and W. Mamdouh, *ACS Omega*, 2022, **7**, 1838–1850.

113 S. Nazarnezhad, F. Kermani, V. R. Askari, S. A. Hosseini, A. Ebrahimzadeh-Bideskan, A. Moradi, R. K. Oskuee, S. Mollazadeh and S. Kargozar, *J. Pharm. Sci.*, 2022, **111**, 2531–2539.
114 A. A. Aboomeirah, W. A. Sarhan, E. A. Khalil, A. Abdellatif, A. S. Abo Dena and I. M. El-Sherbiny, *ACS Appl. Bio Mater.*, 2022, **5**, 3678–3694.
115 M. Kumar, M. Rajput, T. Soni, V. Vivekanand and N. Pareek, *Front. Chem.*, 2020, **8**, 469.
116 D. Elieh-Ali-Komi and M. R. Hamblin, *Int. J. Adv. Res.*, 2016, **4**, 411.
117 A. Anitha, S. Sowmya, P. S. Kumar, S. Deepthi, K. Chennazhi, H. Ehrlich, M. Tsurkan and R. Jayakumar, *Prog. Polym. Sci.*, 2014, **39**, 1644–1667.
118 M. E. Abd El-Hack, M. T. El-Saadony, M. E. Shafi, N. M. Zabermawi, M. Arif, G. E. Batiha, A. F. Khafaga, Y. M. Abd El-Hakim and A. A. Al-Sagheer, *Int. J. Biol. Macromol.*, 2020, **164**, 2726–2744.
119 S. Li, B. Gu, X. Li, S. Tang, L. Zheng, E. Ruiz-Hitzky, Z. Sun, C. Xu and X. Wang, *Adv. Healthcare Mater.*, 2022, **11**, 2102367.
120 Y. Okamoto, K. Kawakami, K. Miyatake, M. Morimoto, Y. Shigemasa and S. Minami, *Carbohydr. Polym.*, 2002, **49**, 249–252.
121 R. Singh, K. Shitiz and A. Singh, *Int. Wound J.*, 2017, **14**, 1276–1289.
122 Y. Shigemasa and S. Minami, *Biotechnol. Genet. Eng. Rev.*, 1996, **13**, 383–420.
123 M. G. Mehrabani, R. Karimian, R. Rakhshaei, F. Pakdel, H. Eslami, V. Fakhrzadeh, M. Rahimi, R. Salehi and H. S. Kafil, *Int. J. Biol. Macromol.*, 2018, **116**, 966–976.
124 P. Fan, Y. Zeng, D. Zaldivar-Silva, L. Agüero and S. Wang, *Molecules*, 2023, **28**, 1473.
125 A. B. Mohd Hilmi, A. S. Halim, H. Jaafar, A. B. Asiah and A. Hassan, *BioMed Res. Int.*, 2013, **2013**, 1–13.
126 F. Wang, S. Hu, Q. Jia and L. Zhang, *J. Nanomater.*, 2020, **2020**, 1–14.
127 X. Liu, L. Ma, Z. Mao and C. Gao, in *Chitosan for Biomaterials II*, ed. R. Jayakumar, M. Prabaharan and R. A. A. Muzzarelli, Springer Berlin Heidelberg, Berlin, Heidelberg, 2011, pp. 81–127, DOI: **10.1007/12-2011-118**.
128 C. Zhang, Q. Zhang, D. Yang, Y. Qiao, B. Wang, J. Yan, Z. Li, Z. Huang, Y. Zhou, K. Hu and Y. Zhang, *Front. Bioeng. Biotechnol.*, 2022, **10**, 1002437.
129 R. A. Masud, M. S. Islam, P. Haque, M. N. I. Khan, M. Shahruzzaman, M. Khan, M. Takafuji and M. M. Rahman, *Materialia*, 2020, **12**, 100785.
130 Y. Haririan, A. Asefnejad, H. Hamishehkar and M. R. Farahpour, *Int. J. Biol. Macromol.*, 2023, **253**, 127081.
131 R. Poonguzhali, S. Khaleel Basha and V. Sugantha Kumari, *Int. J. Biol. Macromol.*, 2018, **112**, 1300–1309.
132 K. Varaprasad, T. Jayaramudu, V. Kanikireddy, C. Toro and E. R. Sadiku, *Carbohydr. Polym.*, 2020, 116025.
133 M. Otterlei, K. Østgaard, G. Skjåk-Bræk, O. Smidsrød, P. Soon-Shiong and T. Espevik, *J. Immunother.*, 1991, **10**, 286–291.
134 N. Zhou, X. Ma, K. V. Bernaerts, P. Ren, W. Hu and T. Zhang, *ACS Biomater. Sci. Eng.*, 2020, **6**, 3310–3326.
135 J. Jia, D. J. Richards, S. Pollard, Y. Tan, J. Rodriguez, R. P. Visconti, T. C. Trusk, M. J. Yost, H. Yao, R. R. Markwald and Y. Mei, *Acta Biomater.*, 2014, **10**, 4323–4331.
136 N. Farshidfar, S. Iravani and R. S. Varma, *Mar. Drugs*, 2023, **21**, 189.
137 H. Babavalian, M. A. Shokrgozar, S. Bonakdar, F. Shakeri and H. Tebyanian, *Trauma Mon.*, 2016, **22**, e64270.
138 J. P. Junker, R. A. Kamel, E. Caterson and E. Eriksson, *Adv. Wound Care*, 2013, **2**, 348–356.
139 R. Ma, Y. Wang, H. Qi, C. Shi, G. Wei, L. Xiao, Z. Huang, S. Liu, H. Yu, C. Teng, H. Liu, V. Murugadoss, J. Zhang, Y. Wang and Z. Guo, *Composites, Part B*, 2019, **167**, 396–405.
140 A. Rezaei and H. Ehtesabi, *Mater. Today Chem.*, 2022, **24**, 100910.
141 F. G. Torres, S. Commeaux and O. P. Troncoso, *Starch/Staerke*, 2013, **65**, 543–551.
142 Y. Ai and J. I. Jane, in *Encyclopedia of Food and Health*, ed. B. Caballero, P. M. Finglas and F. Toldrá, Academic Press, Oxford, 2016, pp. 165–174, DOI: **10.1016/B978-0-12-384947-2.00657-7**.
143 V. S. Waghmare, P. R. Wadke, S. Dyawanapelly, A. Deshpande, R. Jain and P. Dandekar, *Bioact. Mater.*, 2018, **3**, 255–266.
144 M. M. Delavari, I. Ocampo and I. Stiharu, *Micromachines*, 2022, **13**, 2146.
145 A. Tampau, C. González-Martinez and A. Chiralt, *J. Food Eng.*, 2017, **214**, 245–256.
146 C. Su, H. Zhao, H. Yang and R. Chen, *ACS Appl. Bio Mater.*, 2019, **2**, 171–181.
147 S. Nezami, M. Sadeghi and H. Mohajerani, *Polym. Degrad. Stab.*, 2020, **179**, 109255.
148 G. Yaşayan, E. Alarçin, A. Bal-Öztürk and M. Avci-Adali, *Stud. Nat. Prod. Chem.*, 2022, **74**, 367–441.
149 A. Gupta, M. Kowalczuk, W. Heaselgrave, S. T. Britland, C. Martin and I. Radecka, *Eur. Polym. J.*, 2019, **111**, 134–151.
150 J. D. P. de Amorim, C. J. G. da Silva Junior, A. D. L. M. de Medeiros, H. A. do Nascimento, M. Sarubbo, T. P. M. de Medeiros, A. F. d S. Costa and L. A. Sarubbo, *Molecules*, 2022, **27**, 5580.
151 L. Zheng, S. Li, J. Luo and X. Wang, *Front. Bioeng. Biotechnol.*, 2020, **8**, 593768.
152 N. Asadi, A. R. Del Bakhshayesh, S. Davaran and A. Akbarzadeh, *Mater. Chem. Phys.*, 2020, **242**, 122528.
153 L. Zhang, Y. Yu, S. Zheng, L. Zhong and J. Xue, *Carbohydr. Polym.*, 2021, **257**, 117671.
154 M. U. A. Khan, G. M. Stojanović, R. A. Rehman, A.-R. Moradi, M. Rizwan, N. Ashammakhi and A. Hasan, *ACS omega*, 2023, **8**, 40024–40035.
155 Y. Wan, S. Yang, J. Wang, D. Gan, M. Gama, Z. Yang, Y. Zhu, F. Yao and H. Luo, *Composites, Part B*, 2020, **199**, 108259.

156 A. Gupta, S. M. Briffa, S. Swingler, H. Gibson, V. Kannappan, G. Adamus, M. Kowalczuk, C. Martin and I. Radecka, *Biomacromolecules*, 2020, **21**, 1802–1811.
157 H. Adelnia, R. Ensandoost, S. S. Moonshi, J. N. Gavgani, E. I. Vasafi and H. T. Ta, *Eur. Polym. J.*, 2022, **164**, 110974.
158 M. Teodorescu, M. Bercea and S. Morariu, *Biotechnol. Adv.*, 2019, **37**, 109–131.
159 M. Kokabi, M. Sirousazar and Z. M. Hassan, *Eur. Polym. J.*, 2007, **43**, 773–781.
160 E. A. Kamoun, E.-R. S. Kenawy and X. Chen, *J. Adv. Res.*, 2017, **8**, 217–233.
161 S. G. Jin, *Chem. – Asian J.*, 2022, **17**, e202200595.
162 S. M. Nasef, E. E. Khozemy, E. A. Kamoun and H. El-Gendi, *Int. J. Biol. Macromol.*, 2019, **137**, 878–885.
163 S. Song, Z. Liu, M. A. Abubaker, L. Ding, J. Zhang, S. Yang and Z. Fan, *Mater. Sci. Eng., C*, 2021, **126**, 112171.
164 H. Liu, R. Chen, P. Wang, J. Fu, Z. Tang, J. Xie, Y. Ning, J. Gao, Q. Zhong and X. Pan, *Carbohydr. Polym.*, 2023, 121050.
165 G. Nasiri, N. Azarpira, A. Alizadeh, S. M. Zebarjad, M. Aminshahidi, O. Alavi and M. Kamali, *Mater. Today Commun.*, 2022, **33**, 104476.
166 S. Alippilakkotte, S. Kumar and L. Sreejith, *Colloids Surf., A*, 2017, **529**, 771–782.
167 S. F. Gomaa, T. M. Madkour, S. Moghannem and I. M. El-Sherbiny, *Int. J. Biol. Macromol.*, 2017, **105**, 1148–1160.
168 B. Kost, M. Svyntkivska, M. Brzeziński, T. Makowski, E. Piorkowska, K. Rajkowska, A. Kunicka-Styczyńska and T. Biela, *Colloids Surf., B*, 2020, **190**, 110949.
169 S. Sun, H. Li, J. Chen and Q. Qian, *Physiology*, 2017, **32**, 453–463.
170 H. T. J. Gilbert, N. Hodson, P. Baird, S. M. Richardson and J. A. Hoyland, *Sci. Rep.*, 2016, **6**, 37360.
171 S. Chitrattha and T. Phaechamud, *Mater. Sci. Eng., C*, 2016, **58**, 1122–1130.
172 M. Râpă, L. M. Stefan, T. Zaharescu, A.-M. Seciu, A. A. Turcanu, E. Matei, A. M. Predescu, I. Antoniac and C. Predescu, *Appl. Sci.*, 2020, **10**, 2265.
173 M. Ranjbar-Mohammadi, P. Shakoori and Z. Arab-Bafrani, *Int. J. Biol. Macromol.*, 2021, **187**, 554–565.
174 K. K. Chereddy, G. Vandermeulen and V. Préat, *Wound Repair Regen.*, 2016, **24**, 223–236.
175 H. M. E.-S. Azzazy, S. A. Fahmy, N. K. Mahdy, M. R. Meselhy and U. Bakowsky, *Nanomaterials*, 2021, **11**, 2438.
176 T. K. Hunt, W. B. Conolly, S. B. Aronson and P. Goldstein, *Am. J. Surg.*, 1978, **135**, 328–332.
177 P. E. Porporato, V. L. Payen, C. J. De Saedeleer, V. Préat, J.-P. Thissen, O. Feron and P. Sonveaux, *Angiogenesis*, 2012, **15**, 581–592.
178 K. Huang, Z. Jinzhong, T. Zhu, Y. Morsi, A. Aldalbahi, M. El-Newehy, X. Yan and X. Mo, *J. Mater. Chem. B*, 2021, **9**, 1452–1465.
179 L. Sutrisno, H. Chen, T. Yoshitomi, N. Kawazoe, Y. Yang and G. Chen, *J. Mater. Chem. B*, 2022, **10**, 204–213.
180 G. El Fawal, H. Hong, X. Mo and H. Wang, *J. Drug Delivery Sci. Technol.*, 2021, **63**, 102501.
181 A. Bharadwaz and A. C. Jayasuriya, *Mater. Sci. Eng., C*, 2020, **110**, 110698.
182 S. Moeini, M. R. Mohammadi and A. Simchi, *Bioact. Mater.*, 2017, **2**, 146–155.
183 H. A. Rather, R. Thakore, R. Singh, D. Jhala, S. Singh and R. Vasita, *Bioact. Mater.*, 2018, **3**, 201–211.
184 M. Naseri-Nosar, S. Farzamfar, H. Sahrapeyma, S. Ghorbani, F. Bastami, A. Vaez and M. Salehi, *Mater. Sci. Eng., C*, 2017, **81**, 366–372.
185 S. Kouser, A. Prabhu, S. Sheik, K. Prashantha, G. K. Nagaraja, J. N. D'Souza, K. M. Navada and D. J. Manasa, *Int. J. Pharm.*, 2021, **607**, 121048.
186 J. M. Lee, T. Chae, F. A. Sheikh, H. W. Ju, B. M. Moon, H. J. Park, Y. R. Park and C. H. Park, *Mater. Sci. Eng., C*, 2016, **68**, 758–767.
187 A. Keirouz, M. Zakharova, J. Kwon, C. Robert, V. Koutsos, A. Callanan, X. Chen, G. Fortunato and N. Radacsi, *Mater. Sci. Eng., C*, 2020, **112**, 110939.
188 H. Khalid, H. Iqbal, R. Zeeshan, M. Nasir, F. Sharif, M. Akram, M. Irfan, F. A. Khan, A. A. Chaudhry and A. F. Khan, *Polym. Bull.*, 2021, **78**, 7199–7218.
189 M. Ragothaman, A. K. Villalan, A. Dhanasekaran and T. Palanisamy, *Mater. Sci. Eng., C*, 2021, **128**, 112328.
190 M. Ahmadi, M. Mehdikhani, J. Varshosaz, S. Farsaei and H. Torabi, *J. Biomater. Appl.*, 2021, **35**, 958–977.
191 G. Sandri, C. Aguzzi, S. Rossi, M. C. Bonferoni, G. Bruni, C. Boselli, A. I. Cornaglia, F. Riva, C. Viseras, C. Caramella and F. Ferrari, *Acta Biomater.*, 2017, **57**, 216–224.
192 D. Archana, B. K. Singh, J. Dutta and P. K. Dutta, *Carbohydr. Polym.*, 2013, **95**, 530–539.
193 P. T. S. Kumar, V.-K. Lakshmanan, R. Biswas, S. V. Nair and R. Jayakumar, *J. Biomed. Nanotechnol.*, 2012, **8**, 891–900.
194 A. E. Eldeeb, S. Salah, M. S. Amer and N. A. Elkasabgy, *J. Drug Delivery Sci. Technol.*, 2022, **71**, 103292.
195 Y. Fan, W. Wu, Y. Lei, C. Gaucher, S. Pei, J. Zhang and X. Xia, *Mar. Drugs*, 2019, **17**, 285.
196 M. Ansarizadeh, S. A. Haddadi, M. Amini, M. Hasany and A. Ramazani SaadatAbadi, *J. Appl. Polym. Sci.*, 2020, **137**, 48916.
197 D. Z. Zmejkoski, Z. M. Marković, D. D. Mitić, N. M. Zdravković, N. O. Kozyrovska, N. Bugárová and B. M. Todorović Marković, *J. Biomed. Mater. Res., Part B*, 2022, **110**, 1796–1805.
198 W. Wentao, Z. Tao, S. Bulei, Z. Tongchang, Z. Qicheng, W. Fan, Z. Ninglin, S. Jian, Z. Ming and S. Yi, *Appl. Mater. Today*, 2019, **17**, 36–44.
199 S. Faraji, N. Nowroozi, A. Nouralishahi and J. S. Shayeh, *Life Sci.*, 2020, **257**, 118062.
200 A. Góra, M. P. Prabhakaran, G. T. L. Eunice, R. Lakshminarayanan and S. Ramakrishna, *J. Appl. Polym. Sci.*, 2015, **132**, 1–11.
201 P. Zhu, H. Yin, J. Wei, J. Wu, D. Ping and X. Zhang, *Int. J. Biol. Macromol.*, 2023, 125093.
202 D. Sharma, K. K. Bhardwaj and R. Gupta, in *Bionanocomposites in Tissue Engineering and Regenerative Medicine*, ed. S. Ahmed and Annu, Woodhead Publishing, 2021, pp.611–630, DOI: 10.1016/B978-0-12-821280-6.00001-5.

203 J. Chen, Y. Fan, G. Dong, H. Zhou, R. Du, X. Tang, Y. Ying and J. Li, *Biomater. Sci.*, 2023, **11**, 3051–3076.
204 F. Trotta, A. Dony, M. Mok, A. Grillo, T. Whitehead-Clarke, S. Homer-Vanniasinkam and A. Kureshi, *Nano Select*, 2023, **5**, 2300087.
205 D. Warale, M. Shabeena, A. Prabhu, S. Kouser, D. Manasa and G. Nagaraja, *Int. J. Biol. Macromol.*, 2024, **257**, 128628.
206 M. Singh, M. Changmai, T. Ghosh and A. Karwa, *Advanced Materials and Manufacturing Techniques for Biomedical Applications*, 2023, pp.61–101.